TECHNISCHE UNIVERSITÄT MÜNCHEN

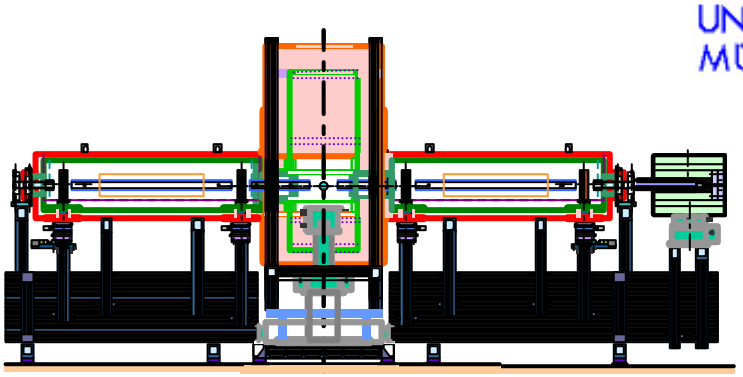

Institute for Experimental Physics
E21

Annual Report 2000/2001

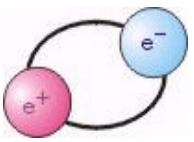

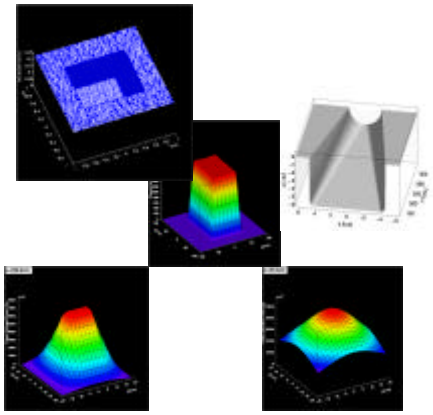

Annual report 2000/2001

Institute for Experimental Physics E21

Annual Report 2000/2001
published: 2.12.2002
Edited by Florian Grünauer, E21
http://www.ph.tum.de/lehrstuehle/E21

Physik-Department E21
Technische Universität München
James-Franck-Strasse
D-85747 Garching, Germany

Phone: +49 89-289-14711
Fax: +49 89-289-14713

INDEX

PREFACE **4**

1 NEUTRON SCATTERING AND MAGNETISM **6**

1.1 MAPPING OF LOW ENERGY EXCITATIONS IN SINGLE-*Q* CHROMIUM 7
1.2 FINCHER-BURKE EXCITATIONS IN SINGLE-*Q* CHROMIUM 8
1.3 SPIN WAVES IN FECR ALLOY AND $[FE_{33.4}CR_{66.6}/AL]_{18375}$ MULTILAYERS 9
1.4 NON-COLLINEAR ORDER IN INVAR IRON-NICKEL ALLOYS 10
1.5 SINGLE ION ANYSOTROPY IN $PR_{0.07}LA_{0.93}NI$ 11
1.6 SPIN GAP IN INTERMEDIATE VALENCE COMPOUND $CE_2NI_3SI_5$ 12
1.7 MAGNETIC STRUCTURE OF THE SPIN-CHAIN COMPOUNDS $CA_{2+X}Y_{2-X}CU_5O_{10}$ 13
1.8 RESEDA SPECTROMETER 14
1.9 MULTIPLE SMALL ANGLE NEUTRON SCATTERING 15
1.10 INTENSITY OPTIMISATION OF A HIGH-RESOLUTION TOF-DIFFRACTOMETER 17

2 NEUTRON RADIOGRAPHY AND TOMOGRAPHY **18**

2.1 DYNAMIC NEUTRON RADIOGRAPHY 19
2.2 APPLIED ENERGY-SELECTIVE NEUTRON RADIOGRAPHY AND TOMOGRAPHY 20
2.3 REPRESENTATION OF THE IMAGE FORMATION IN APPLIED NEUTRON RADIOGRAPHY IN TERMS OF A PSF SUPERPOSITION 21
2.4 OPTIMIZATION OF THE BEAM GEOMETRY FOR THE COLD NEUTRON TOMOGRAPHY FACILITY AT THE NEW NEUTRON SOURCE IN MUNICH 22
2.5 HEAVY CONCRETE AS SHIELDING MATERIAL 23

3 NEUTRON RESEARCH **24**

3.1 INVESTIGATION OF PHOSWICH SCINTILLATORS FOR GAMMA SUPPRESSED ELECTRON DETECTION 25

4 POSITRON RESEARCH **26**

4.1 POSITRON SOURCE BASED ON THERMAL NEUTRON CAPTURE AT THE ILL 27
4.2 SLOW POSITRON BEAM FOR AUGER SPECTROSCOPY 29

5 REACTOR PHYSICS **30**

5.1 ANNUAL REPORT 31

6 ACTIVITIES 2001 ..... **32**

6.1 PUBLICATIONS 2000/2001 33
6.2 LECTURES, COURSES AND SEMINARS 36
6.3 COMMITTEE MEMBERSHIPS 37
6.4 E21 MEMBERS 38
6.5 ASSOCIATED MEMBERS AT FRM-II 39
6.6 GUESTS 39

PREFACE

The Experimental Physics Chair E21 at the Physics Department of the Technische Universität München has witnessed some significant changes during the years 2000 and 2001. On June 1 2000, Peter Böni, formerly employed at the Paul Scherrer Institute in Switzerland, joined the Physics Department in a pre-appointment in order to guarantee a smooth transition in the leadership of the chair of E21 after the retirement of Prof. Wolfgang Gläser on September 30, 2001. This transition was attached further significance by the permanent shut-down of the old Research Reactor Munich FRM (nicknamed “Atomic Egg”) on July 28 2000, that terminated the period where E21 had its “own“ neutron source. It was closely related to this event that the number of members of E21 was reduced significantly due to the transfer of personnel from the FRM to the new high flux research reactor FRM-II which has been organized as a central facility of the whole university. At this opportunity I should like to thank all previous members of E21 for their responsible work at the FRM that has been running without any problems during its nearly 43 years of operation!

From the scientific point of view we have seen some changes in the research priorities of E21. Whereas the group around the technical director of the FRM-II, Prof. K. Schreckenbach, that belongs scientifically to E21 maintains their research in fundamental physics (TRINE) and research with positrons in collaboration with the Universität der Bundeswehr in Munich, the main research topic of the institute has shifted towards magnetism. The future research activities will be devoted to the investigation of chiral fluctuations in one and three-dimensional magnetic structures, the dynamical properties of antiferromagnetic quasi-one dimensional spin chains, and mixed valent systems. In addition we shall investigate magneto-elastic coupling in magnetic multilayers. Clearly, we shall maintain the application oriented research with neutron radiography and tomography as well as our experience in developing new techniques and methods for experiments in neutron scattering. To strengthen this latter point we collaborate closely with Dr. R. Gähler (ZETA Project at IN3) and Dr. F. Demmel (multi detector at IN3) at the Institute Laue-Langevin.

It is clear that the ongoing licensing procedure of the FRM-II puts plenty of work on the shoulders of Profs. K. Schreckenbach and K. Böning and affects strongly their ability to do science. Prof. K. Böning is strongly involved in questions related to the physics of the reactor, including aspects of nuclear performance and safety as well as modifications in the design of fuel elements. In addition, Profs. Schreckenbach and Böning are heavily occupied with paper work that is related to the different safety organisations (TÜV, RSK, SSK) and political institutions (StMWFK, StMLU, BMU, BMWi). The institute E21 is happy about their strong engagement in performing presentations of the FRM-II at national and international scientific meetings and for the public. This is also illustrated by Prof. K. Böning being the Chairman of the International Group on Research Reactors, IGORR.

The reorientation of E21 took place within the rather short period of time of 1.5 years. We have filled the available technical and scientific positions of the institute. Unfortunately, our research is seriously hampered by the delay of the final nuclear permit to run the FRM-II. However, thanks to our good relations with the operators of other neutron sources, in particular with the SINQ facility at Paul Scherrer Institute and with the ILL in Grenoble, we were in a position to continue our research projects more or less successfully. The delay of the nuclear license concerns, in particular one of our most popular and industrially important projects namely the computer tomography with thermal and/or fast neutrons. As a further consequence we are facing the danger loosing our customers - including industry - to foreign facilities.

The projects related to the design and building of the scientific instruments at the FRM-II proceed rather smoothly. The zero-field spin echo spectrometer RESEDA is waiting for more than a year to receive neutrons, and the MIRA beam line very cold neutrons will be operational when the first neutrons are being produced. Most parts of the positron source have been manufactured and even tested and are ready for installation. The tomography facility will be ready by June 2003. There was some delay due to the lack of shielding calculations of neighbouring beam lines. In addition, we should mention that the two instruments PANDA (cold triple-axis) and REFSANS (reflectometer), where E21 has a 10% share, are progressing well, too.

At the Physics Department we have installed during 2001 a physical property measurement system from quantum design that allows the characterization of transport properties like magnetization, susceptibility and specific heat of bulk and multilayer samples. For the preparation of copper-oxide

compounds we acknowledge the excellent collaboration with Dr. A. Erb and Prof. R. Gross at the Walther-Meissner-Institute. In the beginning of the year 2002 we plan to install a D5000 X-ray diffractometer for the characterization of powders and multilayers.

In spite of the serious changes in the organisational structure of E21 during the years 2000 and 2001 we can look back to a rather large number of papers and contributions at international conferences as documented at the end of this report. We should like to thank all members of E21 for their hard work and their efforts on a high level during this transitional stage. In particular I should like to thank Prof. W. Gläser for his continuing support, Prof. K. Schreckenbach who carries the demanding burden to be the technical director of FRM-II and as a scientist at E21 and Prof. K. Böning who is strongly engaged in the nuclear licensing procedure of the FRM-II.

Garching, in June 2002

Peter Böni Klaus Böning Klaus Schreckenbach

I would like to thank Florian Grünauer for editing this report.

Peter Böni

1 NEUTRON SCATTERING AND MAGNETISM

1.1 MAPPING OF LOW ENERGY EXCITATIONS IN SINGLE-*Q* CHROMIUM

P. Böni[1], B. Roessli[2], G.Shirane[3], and S. A. Werner[4]
[1]Technical University of Munich, Physics Department E21, D-85748 Garching, Germany
[2]Laboratory for Neutron Scattering, ETHZ & PSI, CH-5232 Villigen PSI
[3]Brookhaven National Laboratory, Physics Department, Upton, NY 11974, U.S.A.
[4]Department of Physics, University of Missouri, Columbia, Missouri 65211 U.S.A.

The low energy excitations of incommensurate antiferromagnetic Cr have been investigated by means of inelastic neutron scattering with unpolarized neutrons within an energy range –1.5 < E < 9 meV. In agreement with previous measurements by other groups we observe excitations in the transverse spin density phase that appear between the unresolved spin wave peaks at the positions $\mathbf{Q}^{\pm}$ = (1±δ 0 0). In contrast to previous measurements we do not find clear evidence that the Fincher-Burkes modes follow a linear dispersion. (Boni_00_Chrom.doc, II/98 L-23)

Cr is a very fascinating material [1]. At T_N = 311 K it undergoes a transition from a paramagnetic phase to a transversely polarized spin density wave phase (TSDW) characterized by incommensurate wavevectors $\mathbf{Q}^{\pm}$ = (1±δ 0 0). At the spin flip temperature T_{SF} = 121 K a transition to a longitudinaly polarized phase (LSDW) occurs.

The magnetic excitations exhibit many unusual features that are not well understood. In particular, the magnetic modes that originate from the magnetic satellite peaks at $\mathbf{Q}^{\pm}$ exhibit such a steep dispersion that the creation and annihilation peaks cannot be resolved any more. In addition, low energy excitations with a linear dispersion curve that is the same as that of the [ζ00] longitudinal acoustic phonon have been observed in the TSDW phase [2]. Polarized beam experiments, however, shed some doubt about this interpretation [3].

In order to pin down the origin of these Fincher-Burke excitations we tried to measure the temperature dependence of these excitations between 1 meV and 4 meV with very high-resolution. Unfortunately, we did not succeed to observe any clear peaks in constant E-scans. Therefore, we decided to map out as completely as possible the excitation spectrum between the incommensurate peaks up to E = 9 meV using the triple-axis spectrometer TASP at SINQ in the high-resolution mode. The final energy was fixed at 5.573 meV and collimations were open-40-40-open from before the monochromator to the detector, resulting in an energy resolution of 0.25 meV. Figure 1 shows a contour map of the magnetic excitations at T = 230K (0.74T_N) that was constructed by means of 42 constant energy and Q scans. Clearly seen is the strong incommensurate scattering that emerges from the satellite peaks at $\mathbf{Q}^{\pm}$. It consists of contributions from spin wave and phason modes [3]. The spin waves are not resolved due to their extremely high velocity.

The next important contributions to the inelastic scattering appear at the commensurate position (100) at E = 4 meV and 8 meV. These results confirm the work of Fincher et al. [4]. Within the range 4 < E < 8 meV there is an indication that the excitations indeed follow a linear dispersion curve that merges into the incommensurate scattering near E = 8 meV. Polarized beam measurments show that these modes have a longitudinal polarisation [5].

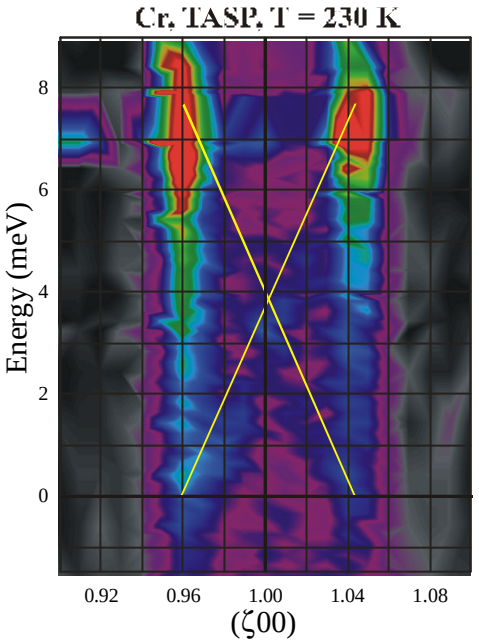

Fig. 1: *Contour map of the excitation spectrum as measured in the transverse spin density wave phase of Cr at T = 230 K. The crossed solid lines indicate the expected dispersion of the Fincher-Burke modes.*

If the dispersion of the Fincher-Burke modes would simply extend linearly from 0 meV at $\mathbf{Q}^{\pm}$ towards E = 4 meV at (100) we would expect significant scattering between 0 and 2 meV similarly as between 6 and 8 meV. This is not observed. Our new results demonstrate that the interpretation of the Fincher-Burke modes should be reconsidered.

[1] E. Fawcett, Rev. Mod. Phys. **60**, 209 (1988).
[2] S. K. Burke, W. G. Stirling, K. R. A. Ziebeck, and J. G. Booth, Phys. Rev. Lett. **51**, 494 (1983).
[3] P. Böni, B. J. Sternlieb, G. Shirane, B. Roessli, J. E. Lorenzo, and S. A. Werner, Phys. Rev. B **57**, 1057 (1998).
[4] C. R. Fincher, G. Shirane, and S. A. Werner, Phys. Rev. B **24**, 1312 (1981).
[5] P. Böni et al. Physica B 267-268, 255 (1999).

1.2 FINCHER-BURKE EXCITATIONS IN SINGLE-*Q* CHROMIUM

P. Böni[1], B. Roessli[2], E. Clementyev[1], Ch. Stadler[1], G.Shirane[3], and S. A. Werner[4]
[1]Technical University of Munich, Physics Department E21, D-85748 Garching, Germany
[2]Laboratory for Neutron Scattering, ETHZ & PSI, CH-5232 Villigen PSI
[3]Brookhaven National Laboratory, Physics Department, Upton, NY 11974, U.S.A.
[4]Department of Physics, University of Missouri, Columbia, Missouri 65211 U.S.A.

For quite some time it has been speculated that the longitudinally polarized Fincher-Burke (FB) modes in Cr follow a linear dispersion curve with a slope that resembles the velocity of sound of the longitudinal acoustic phonon along (ζ 0 0. We have investigated the cross section fo the FB modes with high-resolution neutron scattering and show that wether the dispersion nor the intensity of these modes are compatible with excitations having a linear dispersion curve. (Boni_01_Chrom.doc, II/98 L-23)

Cr is one of the most interesting itinerant antiferromagnets [1]. At the Néel temperature T_N = 311 K, it undergoes a second order phase transition to a transversely polarized spin density wave phase (TSDW) characterized by incommensurate wave vectors $\mathbf{Q}^{\pm}$ = (1±δ 0 0). As a result of the cubic symmetry of paramagnetic Cr, three types of domains are present along the three [100] (Fig. 1).

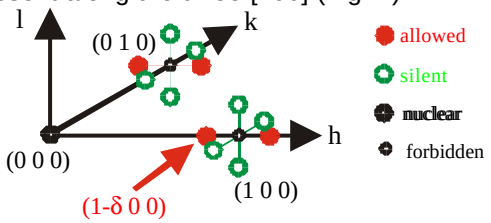

Fig. 1: *Reciprocal lattice of bcc Cr. The filled circles indicate the allowed satellites in the single-**Q** state.*

The magnetic excitations exhibit many unusual features. In particular, the magnetic modes that originate from $\mathbf{Q}^{\pm}$ exhibit such a steep dispersion that the creation and annihilation peaks cannot be resolved. In addition, low energy excitations with a linear dispersion (Fincher-Burke modes) that is the same as that of the [ζ00] longitudinal acoustic phonon have been reported [2]. Recent high resolution experiments indicate that this result may have to be revised [3].

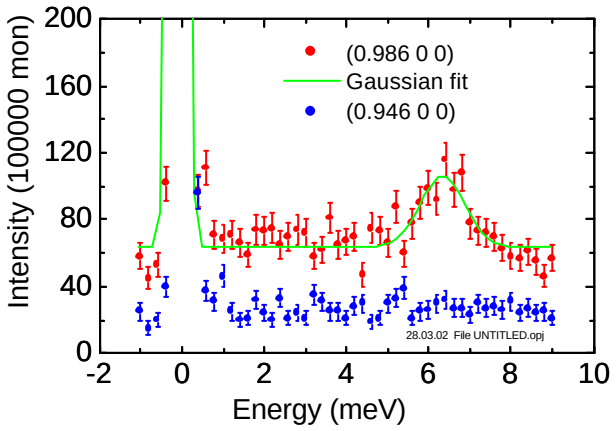

Fig. 2: *Constant-Q scans measured at T = 230 K. The scan at (0.946 0 0) provides the background.*

Using the cold triple-axis spectrometer **TASP** we followed the dispersion of the excitations using constant-Q scans. A typical result **Q** = (0.986 0 0) is shown in Fig. 2 together with the background as measured at (0.946 0 0). Near 6.5 meV a well defined peak is observed. In addition, magnetic scattering is observed that is essentially independent of E. If the FB-modes would follow a linear dispersion we would expect peaks near 2 meV and 5.5 meV. The former peak should be much more intense than the latter because of the thermal population factor $< n+1 >$. We definitely do not observe the low-energy peak. Our measurements confirm also the localized, commensurate excitation at E = 8 meV

In Fig. 3 we show the energy-position of the peaks in constant-Q scans. Clearly, the dispersion of the modes does not extrapolate towards the incommensurate positions $\mathbf{Q}^{\pm}$. The crossed solid lines indicate the expected dispersion of the FB-modes. We conclude that the FB-modes do not follow a linear dispersion.

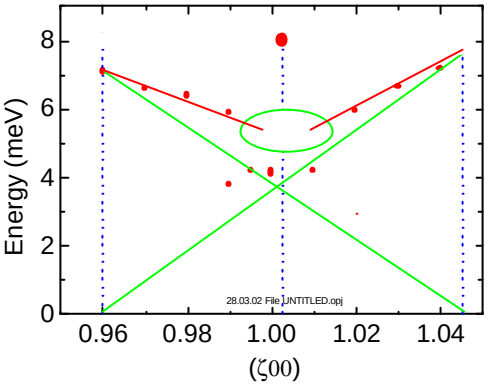

Fig. 3: *The circles indicate the measured data points. Their "dispersion" does not extrapolated to the predicted incommensurate $\mathbf{Q}^{\pm}$-positions.*

[1] E. Fawcett, Rev. Mod. Phys. **60**, 209 (1988).
[2] S. K. Burke, W. G. Stirling, K. R. A. Ziebeck, and J. G. Booth, Phys. Rev. Lett. **51**, 494 (1983).
[3] P. Böni, B. Roessli, E. Clementyev, Ch. Stadler, G. Shirane, and S. A. Werner, Applied Physics A (accepted for publication).

1.3 SPIN WAVES IN FECR ALLOY AND $[FE_{33.4}CR_{66.6}/AL]_{18375}$ MULTILAYERS

P. Böni, M. Senthil Kumar, G. Heigold and M. Horisberger

The measurement of spin wave dispersions allows the determination of magnetic interactions on an atomic scale. In order to study the magnetic coupling between ferromagnetic layers we have tried to measure spin waves in a multilayer composed of 18375 bi-layers [$Fe_{33.4}Cr_{66.6}$(50Å)/Al(50Å)]. Unfortunately, no spin waves were observed, most likely because of an unexpectedly strong softening of the spin waves due to a change of short range order in the sputtered layers. (Boni_00_Multilayer.doc, II/98 L-26)

The coupling of magnetic layers separated by non-magnetic spacer layers has been studied in detail using neutron diffraction. Due to the small sample volumes it was not possible until now to investigate spin wave excitations in these materials. A detailed understanding of the magnetic excitations in multilayers is an interesting task because it will lead to a deeper understanding of the mechanism of the magnetic coupling within and between the magnetic layers. Moreover, it may become feasible to study the transition from *3-d* to *2-d* magnetic behavior.

In a first step we have searched for a ferromagnetic material that has spin waves at such energies that they can be observed in forward scattering. Fig. 1 shows that the $Fe_{33.4}Cr_{66.6}$ alloy ($T_C \cong 380$ K) is an ideal material because spin waves at $Q = 0.04$ Å^{-1} are hard enough to be separated from the elastic peak and soft enough that momentum and energy conservation can be fulfilled in a neutron experiment at 293K.

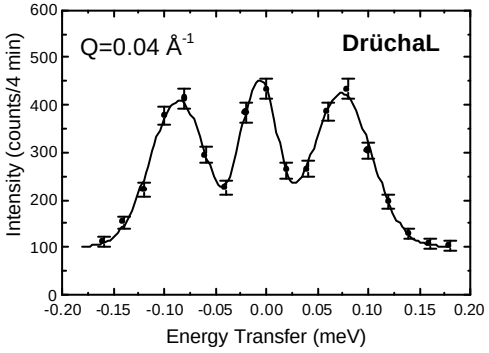

Fig. 1: *Energy spectrum of neutrons scattered from the bulk $Fe_{33.4}Cr_{66.6}$ at 293 K target material.*

In a second step we produced multilayers composed of 18375 bi-layers [$Fe_{33.4}Cr_{66.6}$/Al] with a layer thickness of 50 Å using magnetron sputtering. The structure of the samples was characterized using x-ray diffraction. The inelastic neutron scattering measurements were performed on the triple axis spectrometer TASP at the Swiss spallation source SINQ using a final energy of 2.55 meV.

The constant-Q scan in Fig. 2 does not show any sign of spin waves in the multilayer. Instead, there is an indication of broadening of the elastic line. This result is surprising because the total volume of the magnetic material in the sample ($V = 73.5$ mm^3) is large enough to allow the observation of a magnetic signal. Measurements at low T did not yield a signal either.

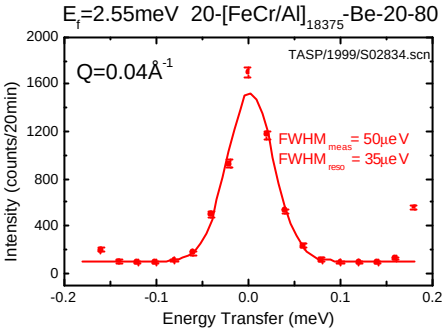

Fig. 2: *Energy spectrum of neutrons scattered from a multilayer composed of 18375 bi-layers [$Fe_{33.4}Cr_{66.6}$/Al] as measured at T = 293 K.*

In order to understand why we did not clearly observe a magnetic signal we have measured the magnetisation of the sample by means of a vibrating sample magnetometer from Quantum Design (Fig. 3).

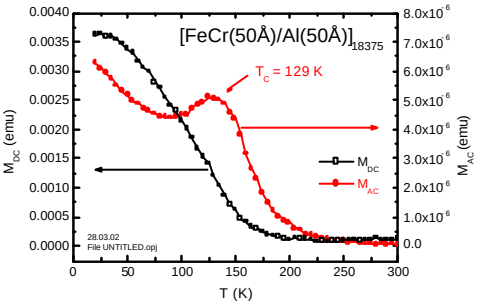

Fig. 3: *DC- and AC-magnetisation of a multilayer composed of 18375 bi-layers [$Fe_{33.4}Cr_{66.6}$/Al].*

The measurements show that the Curie temperature of the multilayer is strongly reduced when compared with the bulk. Therefore, spin waves could not be observed because the data was collected in the paramagnetic phase. However, even at low T spin waves would be hard to observe because the low T_C of the multilayer indicates a $\cong$ 3.5 times lower exchange energy. Hence, excitations at $q = 0.04$ Å^{-1} are expected to occur near 0.02 meV and cannot be resolved anymore. The decrease of T_C in the multilayer is mainly caused be i) a change of the nuclear short range order in the sputtered FeCr layers and ii) proximity effects due to the non-magnetic Al layers. We have determined, that sputtered films of $Fe_{33.4}Cr_{66.6}$ with a thickness $d = 25$ μm have $T_C \cong 200$ K as compared to $T_C \cong 380$ K of the material of the sputter target.

1.4 NON-COLLINEAR ORDER IN INVAR IRON-NICKEL ALLOYS

P. Böni[1], E. Clementyev[1] , and B. Roessli[2]
[1]Technical University of Munich, Physics Department E21, D-85747 Garching, Germany
[2]Laboratory for Neutron Scattering, ETHZ & PSI, CH-5232 Villigen PSI

Invar alloys like $Fe_{65}Ni_{35}$ show almost zero thermal expansion (invar effect) over a wide range of temperature T. The most popular model to explain this effect assumes that the magnitude of the magnetic moments changes with increasing T such that magnetostriction compensates for thermal expansion. Recently it has been proposed that in addition the magnetic moments assume a non-collinear arrangement. In order to prove this model we have performed polarized beam experiments to detect a transverse magnetisation component.(Boni_01_FeNi.doc, II/01 S-23)

Invar alloys have been the subject of numerous investigations using transport measurements as well as neutron scattering. One of the first models to explain the invar effect goes back to Weiss [1], who suggested that there are two possible states for the fcc structure of Fe, namely a state with

- high volume, ferromagnetic
- low volume, anti-ferromagnetic.

Transitions between this two states are suposed to lead to magneto-strictive effects that compensate the thermal expansion. More recent band structure calculations [2] indicate the existence of two states, namely

- high volume, high spin
- low volume, low spin.

Close to the invar concentration, the curves for the respective binding energies differ by a small amount of energy and transitions between them can occur. However, this model cannot be correct because it would lead to a first order phase transition [3].

On the experimental side, the situation is also not understood. The magnetization **M** as calculated from the measured spin wave dispersion curves disagrees strongly with bulk measurements and has lead to the suggestion that a “forbidden” magnetic mode contributes to the strong decrease of **M** with increasing *T* [4]. Recently, a forbidden mode has indeed been observed by means of polarized neutron scattering [5], however, its role with respect to the invar property is not clear.

In general, all theoretical approaches have assumed that the magnetic moments in invar are collinear. Recently, van Schilfgaarde et al. [6] have allowed for the possibility that the moments may exhibit non-collinear spin arrangements. They find, that the transition from the high-spin ferromagnetic configuration to the increasingly disordered non-collinear state occurs as the volume decreases. This model is in good agreement with various experiments, like i) the smooth decrease of the magnetic moment m with increasing *T*, ii) the equilibrium volume is correct, and the iii) the strange behavior of **M** may be understood.

In order to prove the new model we performed neutron scattering experiments with polarization analysis to search for transverse components (spin-flip scattering) of the magnetic moment m and to measure m versus *T*. We reduced demagnetisation effects in the sample by cutting a plate with a thickness of 1 mm from the large single crystal ($8\times8\times18$ mm^3). A vertical field **B** = 30 mT was sufficent to saturate the sample even at room temperature. The neutrons were polarized using a remanent bender before and after the sample. The idea of the experiment was to prove that the transverse component of the magnetic moments increases with increasing *T*.

In order to correct for the *T*-dependence of the flipping ratio determined *R* by measuring phonons and used this number to correct for the elastic. Unfortunately, after submission of the proposal, the experimental space at TASP was dramatically reduced by concrete blocks so that it was not possible to measure the proper phonons. Instead, we investigated the diffuse magnetic scattering from the sample in the forward direction to study a possible influence of the canting on the magnetic correlations. Fig. 1 shows the difference of measurements performed at 655 K and 300 K. Two features are noteworthy, namely the strong peak at $\zeta = ??0.04$ and the dip near $\zeta = ?0.15$. We plan to investigate the polarisation dependence of this scattering in a future experiment.

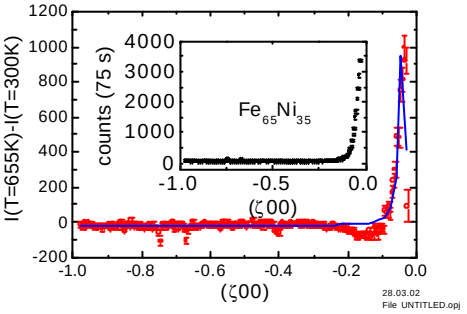

Fig. 2: *Difference of diffuse scattering*

[1] R. Weiss, Proc. R. Soc. London A**82** (1963) 281.
[2] for a review see E.F.Wasserman, in *Ferromagnetic Materials* **5**, Ed. K. H. Buschow and E. P. Wohlfarth,North-Holl.,Amsterdam (1990) 237
[3] M. Schröter, Phys. Rev. B **52**, 188 (1995).
[4] Y. Ishikawa et al., J. Magn. Magn. Mat.**10** (1979) 183.
[5] P. J. Brown et al. J. Phys.: Cond. Matter **8** (1996) 1527.
[6] M. van Schilfgaarde et al., Nature **400** (1999) 46.

1.5 SINGLE ION ANYSOTROPY IN $PR_{0.07}LA_{0.93}NI$

E. Clementyev
Technical University of Munich, Physics Department E21, D-85747 Garching, Germany

The paramagnetic spectral response has been measured in $Pr_{0.07}La_{0.93}Ni$ single crystal along the main crystallographic directions. Two crystal field transitions out of the ground state are clearly seen in the energy transfer range up to 6 meV. The observed anisotropy of these single-ion transitions along with the Q-dependence of the magnetic modes in pure PrNi play a crucial role in understanding of the soft mode-driven magnetic ordering in this compound.

Magnetic ordering mechanism in singlet ground state systems fundamentally differs from one in conventional magnets (see [1] and references therein). The so-called soft mode-driven phase transition is considered as a plausible physical scenario in such systems. A dramatic softening of one of the magnetic modes has been found at the magnetic Bragg point in PrNi [2]. The crystal field (CF) transitions in this system propagate through the crystal due to the exchange coupling between magnetic ions. These dispersive modes are strongly anisotropic due to the exchange interaction between magnetic ions and due to the single-ion anisotropy inherent to Pr ions in low-symmetry crystal surrounding. Discrimination of these two sources of anisotropy is indispensable for getting a quantitative physical picture of the magnetic ordering in PrNi. The main purpose of the present experiment was to determine the single-ion anisotropy of the magnetic excitations in PrNi. The only way to investigate pure single ion effects is to suppress the exchange coupling between Pr ions. That is why a single crystal of diluted compound $Pr_{0.07}La_{0.93}Ni$ was used.

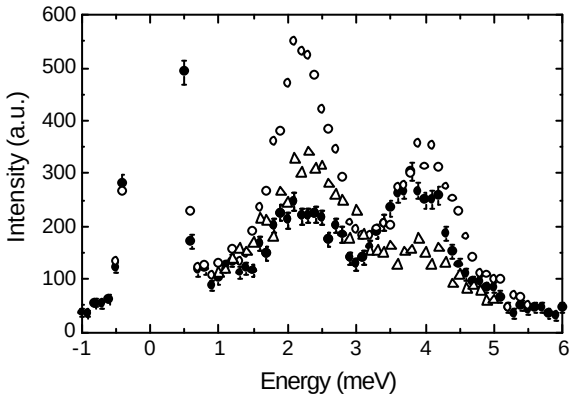

Fig 1: *Neutron spectrum of $Pr_{0.07}La_{0.93}Ni$ measured on RITA-II at T=9K along the directions: [001] - filled circles, [010] - open circles and [100] - triangles.*

Inelastic neutron scattering experiments have been performed on the triple-axis spectrometer RITA-II (single neutron detector configuration). Constant-Q scans were measured at temperatures 9K to 20K for fixed final energy 5.57 meV. A PG graphite filter was placed after the sample to suppress higher order contaminations. The measurements were performed in two scattering planes to access the main crystallographic directions in orthorhombic $Pr_{0.07}La_{0.93}Ni$.

Two well-defined CF transitions out of the ground state were observed along the directions [100], [010] and [001] (see Fig.1). The energies of the peaks are in a good agreement with the high-temperature energy positions of the magnetic modes in pure PrNi [2]. CF transitions indeed appeared to be strongly anisotropic. Using the integrated intensity of the peaks one can estimate the matrix elements of the CF transitions due to the existence of the polarization factor of the magnetic scattering function:

$$S(Q,E) \sim \sum_{i,j} \sum_{a=x,y,z} \left(1-\frac{Q_a^2}{Q^2}\right) |\langle i|\hat{J}_a|j\rangle|^2 \, d(\hbar w + E_j - E_i)$$

where E_i and E_j are the energies of the CF states, Ja - projection of the total angular momentum operator, Q- neutron momentum transfer. The values of the matrix elements along with the parameters of the anisotropic exchange coupling between Pr ions play a crucial role in understanding of the unconventional magnetic ordering in PrNi.

[1] B.R.Cooper in: Magnetic Properties of Rare Earth Metals, ed. R.J.Elliot, Plenum Press (1972), Ch.2, 17.

[2] E.S.Clementyev et al., PSI Scientific Report vol. III (1999) 37.

1.6 SPIN GAP IN INTERMEDIATE VALENCE COMPOUND $Ce_2Ni_3Si_5$

E. Clementyev
Technical University of Munich, Physics Department E21, D-85747 Garching, Germany

The low-energy magnetic scattering intensity was estimated in intermediate valence $Ce_2Ni_3Si_5$. The results are indicative of a possible spin-gap-like magnetic response in this compound. Another important outcome of the measurements is a strong temperature dependence of the phonon spectrum in $Ce_2Ni_3Si_5$.

The paramagnetic spectral response in intermediate-valence (IV) compounds exhibits pronounced anomalies which reflect the unusual dynamics of their magnetic excitations [1]. IV phenomena in $Ce_2Ni_3Si_5$ display unconventional characteristics that may be of great significance for our understanding of this class of materials. The main purpose of the present experiment was to search for a spin gap in the magnetic scattering spectrum of $Ce_2Ni_3Si_5$ at low temperatures. The expected energy scale of the spin gap in such a system is about 10 meV.

The measurements of the inelastic neutron scattering spectra of polycrystalline $Ce_2Ni_3Si_5$ sample (20g) were carried out on the triple axis spectrometer TASP. Since at the time of the experiment its maximum incoming neutron energy was limited we used two different modes. Namely, in the energy transfer range up to 6 meV constant-Q scans were measured at low temperatures for fixed final energy E_f=5.57 meV. To probe higher energies at elevated temperatures the incoming neutron energy was fixed. It both cases a PG filter was placed after or before the sample to suppress higher-order contaminations. The measurements were performed at different Q in the temperature range from 10 to 300K. The magnetic contribution to the spectrum was estimated on the basis of a careful subtraction of the phonon component for low neutron momentum transfer spectra. The phonon spectrum in $Ce_2Ni_3Si_5$ was measured at high Q and high temperatures (phonon scattering dominates in this system at such experimental conditions) and rescaled to the lower values of temperature and neutron momentum transfer.

At low temperature (T=10K) no magnetic scattering intensity was found in the energy transfer range up to 6 meV. This is indicative of a spin-gap like response in $Ce_2Ni_3Si_5$. However to make a definite conclusion on the existence of the gap and its energy one should try to enlarge the energy transfer window and to observe the magnetic contribution to the scattering above 6 meV. The most of the magnetic spectral weight in $Ce_2Ni_3Si_5$ must be located at higher energies.

In addition to the estimation of the magnetic scattering intensity the phonon spectrum of $Ce_2Ni_3Si_5$ was measured for the first time (see Fig.1). A strong temperature dependence of the phonon spectrum was observed. In particular, the peak at about 4 meV which is related to the acoustic phonon mode (modes) in $Ce_2Ni_3Si_5$ demonstrates anomalous temperature dependence. This behavior shows a strong coupling of valence fluctuations and lattice vibrations in this compound.

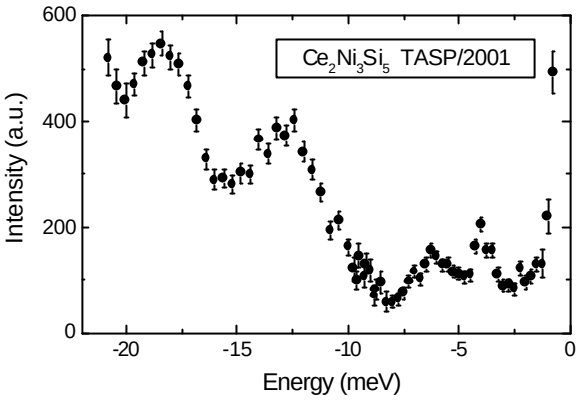

Fig 1: *Background-corrected neutron spectrum of $Ce_2Ni_3Si_5$ measured on TASP at T=300K using fixed incoming energy mode.*

$Ce_2Ni_3Si_5$ in many aspects resembles IV system CeNi [2] with a spin gap in the magnetic excitation spectrum. The valence of cerium strongly depends on temperature in both compounds. $Ce_2Ni_3Si_5$ seems very promising for a detailed study of the anomalous magnetic spectral response and lattice dynamics.

[1] E.Holland-Moritz and G.H.Lander, in Handbook Phys. & Chem. of Rare Earth, v.19, ch.130 (1994).

[2] E.S.Clementyev et al., Phys. Rev. B 57 (14) (1998) R8099.

1.7 MAGNETIC STRUCTURE OF THE SPIN-CHAIN COMPOUNDS $Ca_{2+X}Y_{2-X}Cu_5O_{10}$

A. Mirmelstein [1,2], D. Sheptyakov [3], A. Podlesnyak [2,3], K. Karpinski [4], S. Kazakov [4], P. Böni [1],
[1]Physics Department E21, TUM, James-Frank-str., D-85748, Garching, Germany

[2]Institute for Metal Physics, Russian Academy of Sciences, 620219 Ekaterinburg GSP-170, Russia
[3]Laboratory for Neutron Scattering, ETHZ & PSI, CH-5232 Villigen PSI, Switzerland
[4]Laboratoty for Solid State Physics, ETH Hönggerberg, CH-8093 Zürich, Switzerland

The magnetic structure of the spin-chain compounds $Ca_{2+x}Y_{2-x}Cu_5O_{10}$ as a function of x ($0 \le x \le 1.2$) was measured on the SINQ instrument DMC.

Since the discovery of high T_c superconductivity in cuprate materials, low-dimensional copper-oxide systems have received a great deal of attention. In particular, there is interest in the magnetic properties of spin-chain compounds due to enhancement of quantum fluctuations in one dimension. Recently, a new system $Ca_{2+x}Y_{2-x}Cu_5O_{10}$ has been synthesized which consists only of linear chains and allows a variable doping level ranging from $x = 0$ to $x = 2$ (formal copper valences from +2 to +2.4) [1]. This wide range of hole doping makes this compounds particularly interesting for detailed study of doping-induced dimensional crossover between 3D and 1D. In fact, the undoped compound exhibits long-range AF order with $T_N = 29$ K [2], but as holes are doped into the chains, the magnetic susceptibility and the specific heat data indicate a change from 3D long-range order to 1D chain behavior [3]. Therefore, this compound series is an excellent model for linking experimental and theoretical studies of the spin and charge dynamics in doped low-dimensional copper oxides. The aim of the present study is to characterize the magnetic state of $Ca_{2+x}Y_{2-x}Cu_5O_{10}$ as a function of x by neutron powder diffraction measurements.

The ceramic samples of $Ca_{2+x}Y_{2-x}Cu_5O_{10}$ ($0 \le x \le 1.2$) were prepared at high oxygen pressure (~ 200 bar) as described in [1]. Concentration dependence of the magnetic structure for the compound series was studied at DMC in high intensity mode using λ=2.56 Å. Neutron powder diffraction patterns were recorded in the temperature interval $1.5 < T < 40$ K.

In agreement with the previous results [2], the undoped $Ca_2Y_2Cu_5O_{10}$ experiences an AF ordering at $T_N = 29.5$ K. The Cu ions form an orthorhombic sublattice within the orthorhombic *Fmmm* structure. The magnetic peaks could be indexed within this chemical unit cell with **k** = [0,0,1]. The magnetic moments lie along the *b* direction of the unit cell, i.e. perpendicular to the chain direction [100]. Since the low temperature ordered moment $(0.95\pm0.03)\mu_B$ is close to the free ion value for Cu^{2+}, spin fluctuations are negligible in the undoped material.

The hole doping induced by increase in x leads to the lowering of the Neel temperature and to the uniform decrease of intensities of all the magnetic reflections relatively to the x-independent nuclear peaks (Fig. 1). We thus conclude that in a first approximation the magnetic interactions in the system do not vary with increasing x. In order to understand whether decrease of magnetic peaks occurs due to decrease of the number of spins involved into the long-range order or due to reduction of the effective Cu moment, we have measured the magnetic susceptibility, the high-temperature values of which as a function of x correspond to the spin cancellation of exactly one spin by one extra Ca (Fig. 1). Assuming all the residual (magnetic) Cu ions to be involved into the long-range order, the ratio √(magnetic intensity/Curie constant) gives the upper limit for doping-induced reduction of the Cu magnetic moments (Fig. 1). Therefore, we conclude that the hole doping results in essential reduction of the Cu magnetic moments, most probably due to enhancement of spin fluctuations near the 3D → 1D crossover. Further analysis of the results obtained is in progress.

We thank A. Erb for his help in sample synthesis.

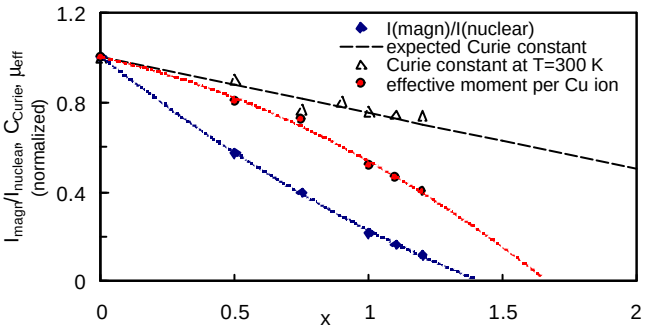

Fig. 1: *Relative variation of intensities of magnetic reflections (normalized first to the intensity of the nearest nuclear reflection), Curie constant at 300 K and effective Cu magnetic moment as a function of x for $Ca_{2+x}Y_{2-x}Cu_5O_{10}$. Dashed line shows the behavior of C_{Curie} correspondent to the spin cancellation of exactly one spin by one extra Ca.*

[1] A. Hayashi; B. Batlogg, R. Cava, Phys. Rev. Lett. **58** 2678 (1998)

[2] H.F. Fong et al., Phys. Rev. B **59** 365 (1999)

[3] M.D. Chabot and J.T. Markert, Phys. Rev. Lett. **86** 163 (2001)

1.8 RESEDA SPECTROMETER

M. Bleuel , R. Gähler
Technical University of Munich, Physics Department E21, D-85747 Garching, Germany

Aktivities in 2001:

- Cabeling of the instrument (Motors, air cussions, air sensors, water, DC- and HF-supply for the Bootstrapcoils)
- Adjustments (with gears) for the detectors are installed
- First tests with the C-box for the resonance-HF-circuit leading to an advanced model (in construction)
- Programming on the instrument-control-programm (drivers for additional devices, component_test_ panels, automated adjustment of the coils and the spectrometer)
- Construction and building of the NSE-Z-coils, with numerical simulation of the MuMetal_joch and test_experiments at the ILL
- Optimising of the B0-Coils (Fortal STS and „Überschleifen“) and produktion of new Coil-bodys, start of the windinds with an improved isolation between the layers
- Building of six very flat rectangular non-magnetic slits
- Control-program for this slits an development of a multiplexer-platine together with the Elektronik-Labor
- Construktion of the guide field for the N-guide together with Christian Schanzer. Building up two 3m models
- Construktion of the inpile for the detectorshield
- Selector-tests with Nikolay Kardilow at the PSI
- Quality measurements of the dance floor (therefore removal and rebuilding of RESEDA)
- First tests of the MuMetallshielding at the final position an adjected simulations
- Removement of damage done to the spectrometer, as much as possible

Actual project state (03.02):

The estimated start of the FRM2 will not be before the end of 2002. Because of this delay of at least 2 years compared to the early time table, all Reseda activitys are streched. It is important to keep the know how and not to break up the team. An additional financing of 50 kEuro for the was granted.

Reseda Spectrometer: Time table

time table Reseda spectrometer	1999			2000				2001		
	4-6	7-9	10-12	1-3	4-6	7-9	10-12	1-3	4-6	7-9
Flipper coils										
base construction										
Magnetic shield										
Positioning devices										
Magnetic fields										
Selector										
Polarizers										
electronics and control										

1.9 MULTIPLE SMALL ANGLE NEUTRON SCATTERING

T. Hils, R. Gähler, and P. Böni, Technical University of Munich,
Physics Department E21, D-85748 Garching, Germany

Die Neutronen-Klein-Winkel-Streuung (SANS) ist im Lauf ihrer Entwicklung zu einem bedeutenden Verfahren zur Untersuchung von Nano-Strukturen (ca. 1 bis 1000 Å) in der Festkörperphysik, der Chemie und Biologie geworden. Damit lassen sich die „globalen Strukturen" großer Molekülverbände in ihrer natürlichen Umgebung untersuchen, z.B. Proteine in physiologischer Lösung.

Im Rahmen einer Diplomarbeit am Lehrstuhl E21 sollen die wesentlichen experimentellen Eigenschaften wie z.B. Auflösung und Intensität einer konventionellen SANS-Maschine mit einer Anordnung verglichen werden, bei der mittels zweier periodischer Lochmasken (Lochdurchmesser d typisch 1mm, Lochabstand ca. 2,5 mm, Anzahl der Lochblenden $N_{1,2}$ ca. 10-100) eine inkohärente Überlagerung vieler „kleiner" höchstauflösender SANS-Maschinen erreicht wird (Abbildung 1). Die Anzahl der Überlagerungen ergibt sich aus dem Produkt der ausgeleuchteten Lochblenden $N_1 \cdot N_2$. Die prinzipielle Idee hierbei ist, die aufgrund der kleinen Lochblende (bestimmend für hohe Auflösung) stark verminderte Intensität durch die inkohärente Überlagerung vieler Raumwinkelanteile zu kompensieren.

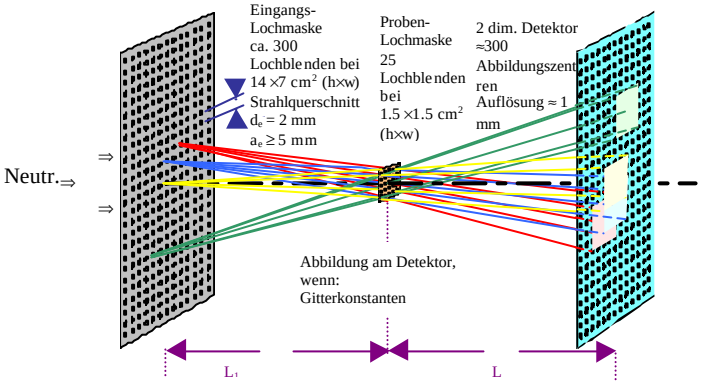

Abb. 1: MSANS als höchstauflösende Option für bestehende SANS-Instrumente bei sehr grossem Strahlquerschnitt (14 x 7 cm²)

Auflösung:
Unter der idealisierenden Annahme, dass keine räumliche Überlagerung der einzelnen Beugungsmuster am Detektor stattfindet, d.h. keine Entfaltung der Streufunktion notwendig ist, ergibt sich für die Auflösung der gleiche Term (Gl. 1) wie beim konventionellen SANS.

q- Auflösung von SANS

$$\Rightarrow \Delta q^2 \approx \frac{k^2}{12}\left(\left(\frac{d_E}{L_1}\right)^2 + \left(\frac{d_S}{L_2}\left(\frac{L_1+L_2}{L_1}\right)\right)^2 + \left(\frac{d_D}{L_2}\right)^2 + \left(\frac{\Delta l}{l}\cdot q\right)^2\right)$$

Intensität:
Die Intensität von MSANS wird im wesentlichen durch den Faktor $N_1 \cdot N_2$ bezogen auf die Intensität eines entsprechenden SANS gleicher Auflösung und Eintrittsblende vergrößert.
Gewinnfaktor gegenüber SANS bei gleicher Auflösung: $\Rightarrow \frac{A_S}{L_1^2}, \frac{A_D}{L_2^2} = const.$

$$G = \frac{Z_{MSANS}}{Z_{SANS}} = N_1 \cdot N_2 \cdot \frac{A_{S\,MSANS}}{A_{S\,SANS}}$$

(bei unterschiedlicher Eintrittsblende)

$$Z_D^{MSANS} \propto N_1 \cdot N_2 \cdot \frac{A_E}{L_1^2} \cdot A_S \frac{A_D}{L_2^2}$$

$N_{1,2}$: Anzahl Lochblenden in Lochmaske 1 bzw. 2
A_E : Querschnittsfläche einzelner Lochblende (Eintrittsblende)
A_S : Querschnittsfläche einzelner Lochblende (Probe)
A_D : Fläche eines Detektorelements
L_1 : Abstand Eingangsblende - Probe
L_2 : Abstand Probe - Detektor

Beispielgeometrie:

	SANS	MSANS
Strahlprofil	120.10 mm²	120.10 mm²
Probengröße	10 mm²	10 mm²
N_1	--	50
N_2	--	6
A_S	25 mm²	1 mm²
Gewinn (MSANS/SANS)	12	

Für die o.g. experimentellen Bedingungen lässt sich mit MSANS damit bei gleichen Längen L_1, L_2 eine Verbesserung der Intensität um den Faktor G ≈12 erzielen.

Gravitationskorrektur

Die aufgrund unterschiedlicher Neutronengeschwindigkeiten auftretenden Abweichungen in der Flugbahnkurve im Gravitationsfeld machen eine Korrektur dieses Effekts notwendig. Sie wird über ein Glasprisma mit Öffnungswinkel γ erreicht.

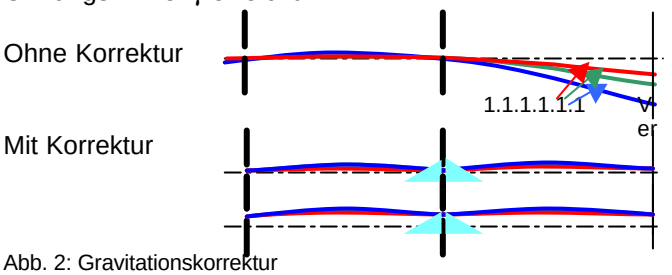

Abb. 2: Gravitationskorrektur

Zusammenfassung - Vorteile:
- Erhöhung der räumlichen Auflösung um Faktor 5-10 bei vergleichbarer Intensität
- Kleine Probengröße (1.5 × 1.5 mm²) möglich
- Keine beam-stops im Detektor notwendig, da keine lokale Sättigung erwartet wird
- Räumliche Auflösung des Detektors kann über gesamte Breite verwendet werden

Technologische Herausforderung und gepl. Schritte:

- SANS Detektor mit 1 mm Auflösung über gesamte Fläche ($\approx 50 \times 50$ cm²)
- Anfertigung der Lochmasken im Hinblick auf neutronenoptisches Verhalten (z.B. Absorption)
- Herstellung der Prismen zur Gravitationskorrektur
- Große Strahlquerschnitte, Querschnittsfläche (14 $\times$ 7 cm²)
- Aufbau eines Testexperiments
- Anfertigung zweier Lochmasken aus Cadmium für erste Tests. Zur Vermeidung von Streuung an der Lochinnenseite müssen die Löcher leicht konisch (ca. 1°) verlaufen.

1.10 INTENSITY OPTIMISATION OF A HIGH-RESOLUTION TOF-DIFFRACTOMETER

F. Demmel[1], Ph. Bernhardt[1], A. Magerl[1], E. Steichele[2]
[1]Universität Erlangen-Nürnberg, Lehrstuhl für Kristallographie und Strukturphysik, Bismarckstr. 10, D-91054 Erlangen
[2]TU München, Physikdepartment E 21, D-85747 Garching, Germany

Neutron time-of-flight (TOF) diffraction is an alternative to the classical double-axis diffraction (DAS) technique. It is the only method for pulsed neutron sources, but it is also a very advantageous technique for steady state reactors. With stationary detectors a large solid angle from the sample to the detectors and therefore large intensity gains compared to the classical method can be realized. In a backscattering geometry the resolution can be very good and the optimum matching of intensity and resolution to the physical problem to be studied can be obtained more easily than with the classical DAS technique. Based on the experience with a prototype TOF diffractometer at the old FRM-I [1] a combination of a high resolution TOF diffractometer with a backscattering spectrometer was proposed for the new reactor FRM-II in Garching. In the present study the diffractometer part, as shown in fig.1, has been optimized. The instrument has been foreseen to be located at one of the neutron guides looking onto the cold source through beam tube SR1. The neutron pulses will be created by a counter-rotating double disk chopper. The second and third chopper cut out the needed wavelength band and the correct number of pulses to avoid frame overlap at the detector. For a good TOF resolution a long flight path (about 80 m), ending in the reactor hall of the old FRM-I, was chosen. The concentric detector is positioned in backscattering geometry around the end of the guide.

In a TOF experiment the lattice parameter d is connected via the Bragg equation with the flight time t, the flight path length L and the scattering angle 2θ by: $2d*\sin\theta = (h/m)*(t/L)$ with h the Planck constant and m the neutron mass. The relarive resolution for the lattice parameter d is then given by: $(\Delta d/d) = \sqrt{((\Delta L/L)^2+(\Delta t/t)^2+(\cot\theta*\Delta\theta)^2)}$, if the deviations are all Gaussian distributed. If we want a resolution in d ~ 2 A of $2*10^{-4}$ and assume equal contributions from all deviations we get, with a flight path of 80 m, a pulse width of 10 μs, a flight path length uncertainty of 9 mm, a scattering angle of θ = 88.6°. In a better approximation we took, instead of Gaussian distributions, the variances of our real distributions and got the relative resolution as function of wavelength, where we used only the geometrical parameters of our set-up. Then an expression for the intensity in the detector was derived with the geometrical data of our instrument, with the neutron spectrum of the cold source and the input geometry of the guide and with the crystallographic data as relevant for powder diffraction. For intensity optimisation with a given resolution the thickness of the sample, the width of the chopper slits and the distance from the guide end to the sample are free parameters, the best values of which were found by the Lagrange multiplicator method. Intensity can be improved by a greater detector, but the gain as a function of detector size comes to saturation and an intensity gain of 20 % may need a 250 % larger detector. The spectrum at the sample, the diffraction line shape and the intensity as function of detector size, as calculated by our analytical formulas, were cross-checked by Monte Carlo simulaions with very good agreement of the two data sets. Details of this work can be found in reference [2].

[1] E. Steichele, P. Arnold Phys. Lett 44A (1973), 165-166
[2] F. Demmel, Ph. Bernhardt, A. Magerl, E. Steichele, NIM in Phys. Res. A 459 (2001) 265-272

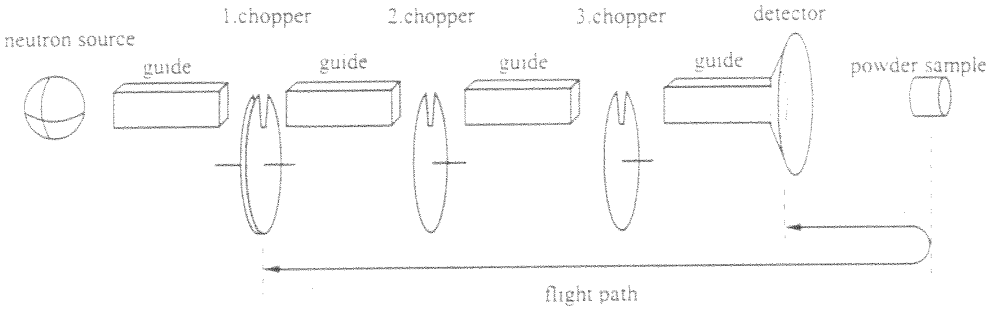

Fig. 1. A sketch of the proposed high-resolution ToF diffractometer for the FRM-II.

2 NEUTRON RADIOGRAPHY AND TOMOGRAPHY

2.1 DYNAMIC NEUTRON RADIOGRAPHY

J. Brunner[a], G. Frei[b], E. Lehmann[b], B. Schillinger[a]
Technical University of Munich, Physics Department E21, 85747 Garching, Germany
Paul Scherrer Institut,5232 Villigen, Swizzerland

Neutron Radiography is well established technique, which is applied very successful for non destructive testing at many institutes. The reached resolution is 100 µm for the best systems and the detection efficiency of a neutron get better than 10%. An aim for the future is to allow an observation of time dependent phenomena with a similar resolution and similar contrast. We built a detector for dynamic neutron radiography and investigated a running combustion engine as a first test sample.

It was planed to use a new gateable CCD camera with image intensifier from the Paul Scherrer Institute for dynamic neutron radiography. Because the camera manufacturer was not able to deliver it in time it was necessary to built our own detector system.
For dynamic neutron radiography there are two quite different techniques:

- using a camera with a high frame rate (i. e. a video camera with 30 f/s) which defines the time resolution
- synchronizing the time dependent phenomena with the position sensitiv detector and summing the single frames up. In that case the gating time determines the time resolution

A detector was built, having both possibilities. Since the costs should not exceed a certain limit, a 8 bit CCD camera Basler 302fs with 758x582 pixels was bought and a commercial night vision equipment was used for an image intensification.
The neutron radiography detector is shown in **Fig. 1**. The design of the detector is described in more detail (See **[1]**).

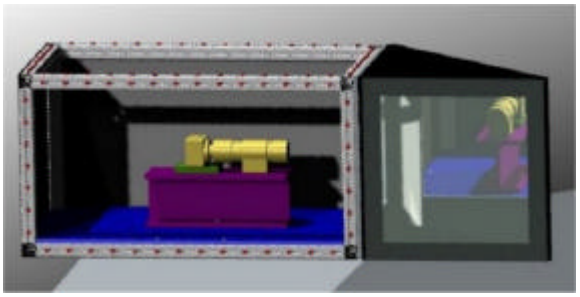

***Fig. 1**: Detector system for dynamic neutron radiography used for the measurements at PSI*

The gating and the opening times of the CCD camera were controlled by a sensor on the object and a self developed delay electronics.
As a first test sample a combustion engine was used, since similar experiments were already performed and our future aim will be the visualization of the fuel injection process **[2]**.
Together with the institute of mechanical engineering at the TU-Munich a test stand for running the combustion engine up to 600 rpm with a electric motor was developed and built.

Fig. 2: Test stand for the combustion engine

The first measurements were performed at PSI. Gating and opening times of the CCD camera were controlled by a sensor on the object and a self developed delay electronics. The neutron radiography images were taken at 200 rpm and each cycle was divided into 30 steps of 10 ms per frame. 500 synchronized neutron radiographs were summed up to one image with a corresponding gating time of 5 s (See **Fig. 3**) .

***Fig. 3**: A single frame (left) contains only 14 graylevels and a summed NR-image after processing (right).*

[1] B. Schilllinger, “Neue Entwicklungen zu Radiographie and Tomographie mit thermischen Neutronen“, Doktorarbeit an der technischen Universität München

[2] M. Balasko, “Neutron radiography visualization of internal processes in refrigerators”, Physica B: Condensed Matter, Volumes 234-236, 2 June 1997, Pages 1033-1034

2.2 APPLIED ENERGY-SELECTIVE NEUTRON RADIOGRAPHY AND TOMOGRAPHY

N. Kardjilov (TU Munich), S. Baechler (Univ. Fribourg & PSI), G. Frei (PSI), E. Lehmann (PSI)

The attenuation coefficient for monoenergetic cold neutrons changes quite drastically at the Bragg cut-offs for many solid materials due to the coherent neutron scattering by the crystal lattice. In many cases, the variation in the total cross section for the corresponding element is significant and this behavior can be exploited to achieve material discrimination in radiography and tomography images by modifying the spectrum of the applied neutron beam.

The radiography set-up was constructed as it is shown in fig. 1. The velocity selector was placed at the end of the curved PGA neutron guide, which faced the cold source at the spallation source SINQ, PSI. Thus this beam position gave the opportunity to perform radiography and tomography experiments at low neutron energies (so-called cold neutron radiography) where the attenuation coefficients for many crystalline materials change drastically[1].

Fig. 1: *Positioning of the velocity selector at the PGA beam line for neutron radiography and tomography purposes.*

The characteristics of the neutron beam at the end of the guide and the detection system itself have been described in detail elsewhere [2].
First a multi-component test sample was investigated at different wavelengths in the range of 2.6 to 9.6 Å. The object consisted of a stack of plates from different materials with a constant thickness of 5 mm as it is shown in fig. 2a.

Fig. 2: *a) Structure of the used radiography test sample; b) Division of pictures obtained at 3.0 Å and 4.3 Å, and c) at 6.4 Å and 7.5 Å*

Using exponential attenuation law for neutrons – $\ln(I/I_0)=\Sigma d$, the attenuation coefficient Σ for each material depending on the neutron wavelength was calculated. The calculated values were compared in fig. 3 with tabulated cross-section values for Cu available in ref. [3]. A good agreement with the tabulated data was found. In addition, the graph in fig. 3 shows that the attenuation coefficient for Cu is the same at 3.0 Å and 4.3 Å. Then the division of the pictures obtained at these two neutron wavelengths made Cu "invisible" in the resultant picture as it is illustrated in fig. 2b. Finally the same procedure was performed in fig. 2c where the Al and Pb plates became "transparent".

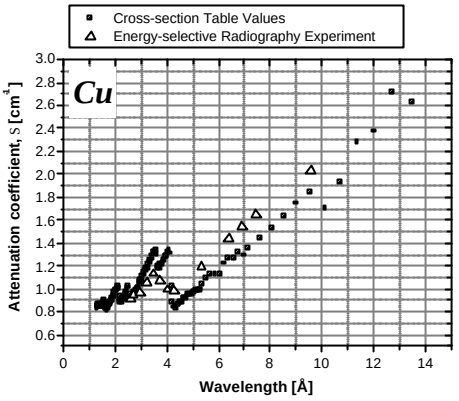

Fig. 3: *Comparison between tabulated and calculated data of energy dependent attenuation coefficients for Cu*

The energy selective technique was used to study the spectral dependence of the quality of the reconstructed tomography slices. For this purpose a simple test sample was prepared. In a 1-cm-thick aluminum cylinder holes with different diameters were bored parallel to the cylinder vertical axis and filled with different metal powders. The reconstructed horizontal slices for tomography experiments performed at three different neutron wavelengths are shown in fig. 4.

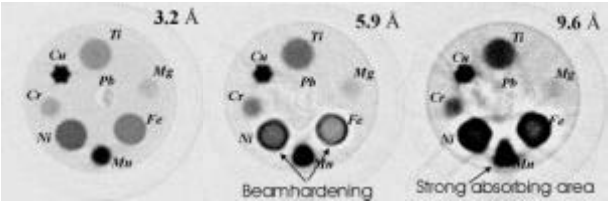

Fig. 4: *Horizontal reconstructed slice of a test sample for tomography experiments performed at three different neutron wavelengths.*

From the presented reconstructions can be seen that at larger neutron wavelengths the contribution of some artefacts as beam hardening or distortions due to existence of strong absorbing areas is of great importance.

[1] N. Kardjilov et al., Applied Radiation and Isotopes. (submited, 2001)
[2] S. Baechler et al.,Nucl. Instr. and Meth.(2001) in press
[3] http://www-nds.iaea.or.at/exfor/

2.3 REPRESENTATION OF THE IMAGE FORMATION IN APPLIED NEUTRON RADIOGRAPHY IN TERMS OF A PSF SUPERPOSITION

N. Kardjilov (TU Munich), E. Lehmann (PSI), P. Vontobel (PSI)

The process of a neutron radiography image formation can be described in terms of a Point Spread Function (PSF) superposition. This way all distortions in the radiography picture obtained at different experimental conditions can be described as alterations in the corresponding PSF. The scattered neutrons are one of the main sources of such distortions. Monte Carlo simulations (MCNP-4b code) were performed for calculations of PSF for different materials, thicknesses and distances between sample and detector.The simulations were used as a base for further corrections in radiography images.

The signal obtained in the radiography measurement can be considered as a result of superposition of three different mechanisms of interaction between the neutrons and the investigated sample. The neutron flux after the interaction can be divided into the following corresponding components: a) *collided* flux - component of neutrons that reach the detector after being scattered in the sample; b) *uncollided* flux - component of neutrons that penetrate the sample without interacting with it; and c) *unmodified* neutrons that reach the detector without penetrating the sample, i.e. the direct beam area where the investigated sample is not presented. A graphic representation of this model for a parallel neutron beam is shown in fig.1.

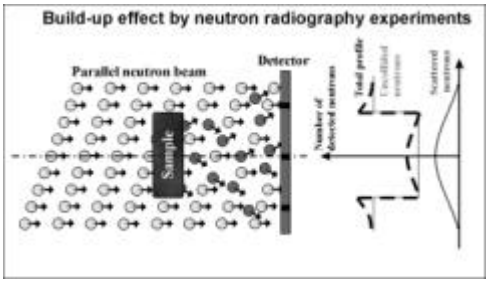

Fig.1 *A schematic representation of the image formation process*

The process of a neutron radiography image formation can be described in terms of a Point Spread Function (PSF) superposition for a given space discretization. If one uses the same discretization for the detector as well as for the neutron source then the PSF can be represented as a sum of two parts - the collided and uncollided neutrons for one emitting pixel. The neutron distribution corresponding only to the collided part of the PSF can be defined as Point Scattered Function (PScF). A Monte Carlo model was used for a calculation of the PScF for homogenous materials. The geometry of the used model is shown in fig. 2.

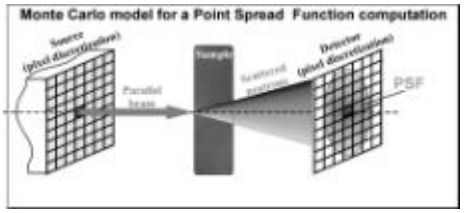

Fig. 2 *The used Monte Carlo model for a calculation of the PScF*

A correction algorithm based on the subtraction of the calculated PScF superposition for the sample area from the experimental image was developed. The test of the algorithm was performed on a sample with an inhomogeneous thickness - a Plexiglas step wedge investigated at 5mm distance from the detector, fig. 3. For each thickness the corresponding PScF was calculated previously. In the correction procedure for different steps, different PScF were used. The intensity profile through the corrected wedge was compared with the profile of the same step wedge investigated at a larger distance (5 cm) between the sample and the detector where the contribution of scattering neutrons is not of a great importance. A good agreement between the corrected and the experimental data was observed.

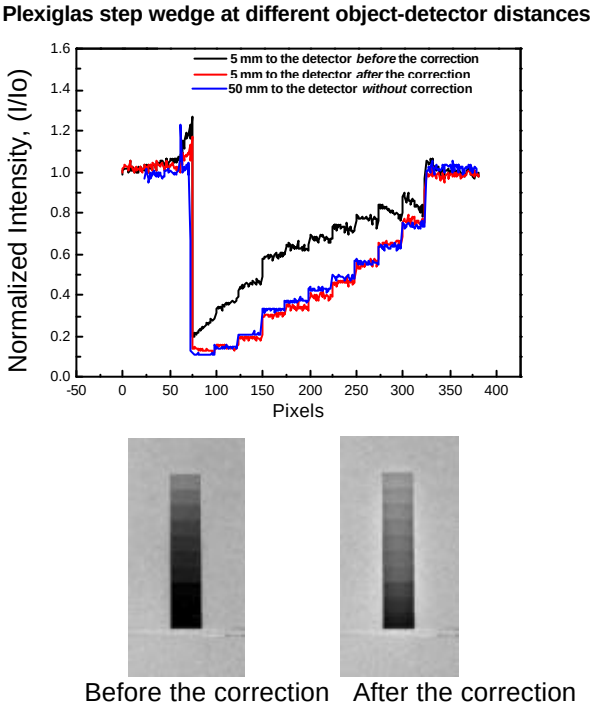

Fig. 3 *An example for a build-up correction of a Plexiglas sample (step wedge)*

The presented correction method of the contribution of the scattered neutrons in neutron radiography images can be used in quantitative radiography analysis. The method allows corrections for homogeneous objects with various shapes and different thicknesses.

2.4 OPTIMIZATION OF THE BEAM GEOMETRY FOR THE COLD NEUTRON TOMOGRAPHY FACILITY AT THE NEW NEUTRON SOURCE IN MUNICH

F. Grünauer, B. Schillinger, E. Steichele
Technische Universität München, Physik-Department E21

One of the very interesting applications at Munich´s New Neutron Source will be neutron tomography. It will be used both for research and industry. The D_2O moderated high flux reactor will provide thermal neutrons for the structural analysis of specimen up to the size of 1m. A central problem is the design of the beam geometry, especially the layout of the collimator and the aperture. Calculations were carried out in order to get an optimal beam geometry, taking into consideration an extended source, low beam divergency and high flux in the detector plane.

At Munich´s tomography facility we have no direct sight to the core. By this we achieve a low fraction of fast neutrons and gamma rays in the beam tube. The beam tube is directed to the cold source. The ´fictive´ neutron source for our facility is the entrance window of the beam tube, that has a rectangular shape of 18cm height and 12cm width and a nearly homogeneous source distribution. The maximum of the spectral neutron distribution is at 2.5meV [1]. The decision to use cold neutrons was taken in order to get a high flux around Bragg cut offs. This enables energy selective radiography. The distance between source and detector plane is some 21m. Due to restrictions arising from the building and other experiments this distance can be varied not more than ±1m. The beam will be shaped by a collimator, that has four purposes:

- to improve the resolution (L/D ratio)
- to cut the beam to the desired rectangular field size of 40cm x 40cm in the detector plane
- to keep the flux in the penumbra region as small as possible
- to keep the level of scattered neutrons at a minimum (radiation protection, noise level)

The collimator should confine the beam as tightly as possible in order to get low noise and to meet the requirements of radiation protection. On the other hand no part of the collimator should hamper source neutrons which contribute to the beam.

Obviously, having a rectangular source and a circular aperture, no simple geometry of the collimator can fulfill all requirements. A simple geometry would be a cone (fig. 1), a collimator with rectangular cross section, or any other arrangement which can be easily machined.

The layout of a collimator with optimal beam adjustment for our facility is shown in fig. 1. Before having it machined we did some Monte Carlo calculations to prove whether it really pays to realize the somewhat strange inner shape of the collimator. The Monte Carlo calculations were carried out by help of MCNP [2]. The results of the calculations clearly showed that the beam adjusted collimator is useful in our geometry: The beam edge is sharper and the contribution of scattered neutrons and leakage neutrons in the penumbra region is significantly lower (two orders of magnitude) compared to a cone shaped collimator (fig.2). The line profile within the beam is not influenced by the collimator.

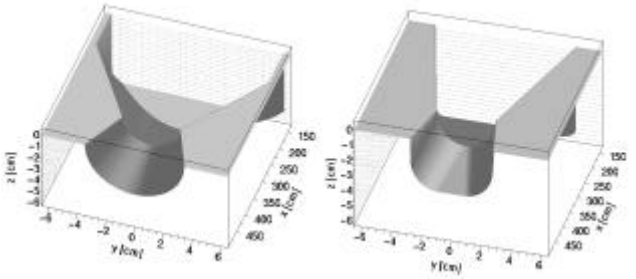

Fig. 1: left hand side: cone shaped collimator (horizontal cut); right hand side: beam adjusted collimator (horizontal cut)

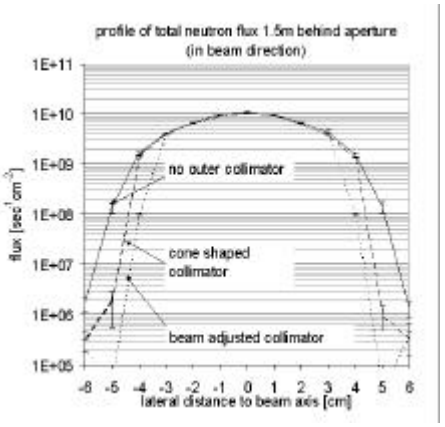

Fig. 2: Neutron flux profile in a distance of 1.5m behind the aperture (in beam direction)

Sometimes parallel collimators (honey comb collimators) are used in radiography [3]. This type of aperture/collimator has no advantages when applied in the given geometry. A parallel collimator with a length of 2.7 m and a channel width of 5 mm was calculated. The small field size in the detector plane is prohibitive for a series of planned experiments with large specimen.

2.5 HEAVY CONCRETE AS SHIELDING MATERIAL

F. Grünauer
Technische Universität München, Physik-Department E21

Concrete is the material used most widely as shielding material. It attenuates both neutron and gamma radiation well, but the effectiveness varies with the composition of the concrete. Several additives for improvement of the shielding power have been proposed. Heavy materials like iron are used to reduce the neutron energy by inelastic scattering to a level, where the cross sections of light elements for elastic scattering are higher. In addition heavy materials attenuate the gamma radiation. The water in the concrete and its additives is used for moderation. Neutron capture at hydrogen is unwanted because of the production of 2.2 MeV gammas. For thermal neutron absorption, materials like boron containing minerals (B^{10}: $?_{(n,?)}$=3837barn) are used. An efficient combination of macroscopic cross sections for:

- inelastic scattering
- elastic scattering
- absorption

is therefore essential for neutron attenuation in heavy concrete.

We intend to use a standard composition of heavy concrete for the new neutron radiography station. Additives are hematite (Fe_2O_3), colemanite ($Ca_2B_6O_{11}\cdot 5H_20$), and steel resin. The composition is shown in fig.1.

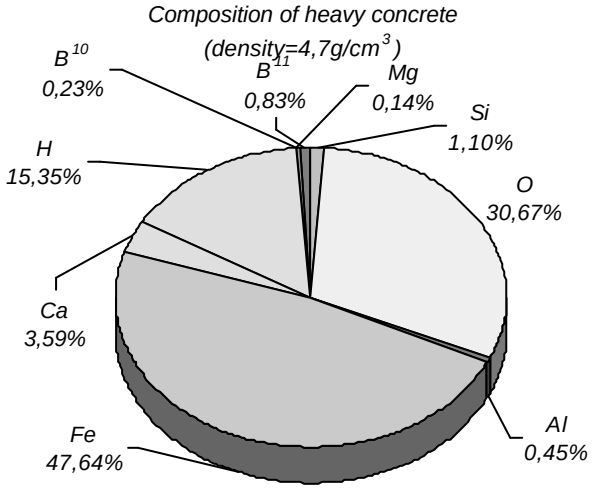

Fig. 1: Composition of heavy concrete

An interesting question is, whether this composition is the optimum for our facility, or if a variation of mixture can improve the shielding power. Monte Carlo calculations were carried out using an isotropic point source in the middle of a sphere (radius = 60 cm) consisting of heavy concrete. The source spectrum is shown in fig. 2. The dose is calculated at the surface of the sphere. The composition was varied by stepwise substitution of steel by the same volume of colemanite. The step width is the volume of 100 kg colemanite. To find the optimal boron content, a mineral that does not contain boron was added to the composition in the same way: serpentine ($Mg_3Si_2O_5(OH)_4$). This mineral is widely used as additive because of its high hydrogen content (in addition it is useful under certain conditions, because it enables the concrete to withstand high temperatures) .

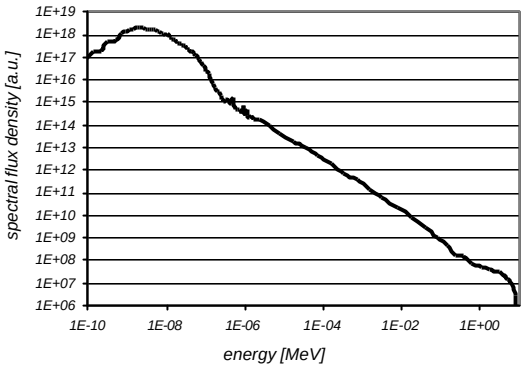

Fig. 2: Neutron source spectrum

The dose of neutron radiation and of generated gammas as function of the colemanite and serpentine content is shown in Fig. 3.

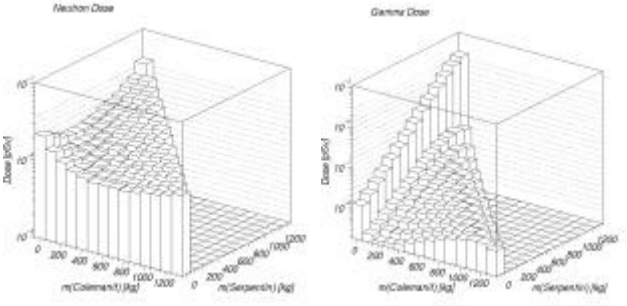

Fig. 3: Neutron dose (left hand side) and dose of generated gammas (right hand side) behind 60 cm of heavy concrete as function of its colemanite and serpentine content, resp.

The standard concrete has a colemanite content of 100 kg. The results clearly indicate, that its composition is not the optimum. The minimal neutron dose can be achieved for 600 kg in theory. On the other hand mixtures with such high amounts of additives tend to be astable or are not able to set. Colemanite contents of up to 400 kg/m^3 are reported to be feasible.

The lowest dose of generated gammas can be achieved with 200 kg of colemanite, but the biggest dose decrease occurs between 0 an 100 kg colemanite. Anyway, serpentine weakens attenuation of neutron radiation as well as of generated gamma radiation. With the ´standarad´ composition we are very close to the theoretical optimum, however.

3 NEUTRON RESEARCH

3.1 INVESTIGATION OF PHOSWICH SCINTILLATORS FOR GAMMA SUPPRESSED ELECTRON DETECTION

Christian Plonka
Technische Universität München, Physik-Department E21

The experiment TRINE investigates time reversal invariance in free polarized neutron beta decay. The low energy electrons (<780 keV) and the protons as the decay products have to be detected in coincidence and with respect to the neutron spin direction. TRINE uses multi wire proportional chambers (MWPC) together with scintillators for electron detection and low noise PiN diodes for detection of the accelerated protons. The MWPCs give us a sufficient gamma suppression and spatial information about the electrons. This was exploited for the data analysis of the last TRINE beam time in 2000 at the Institut Laue Langevin (ILL) in Grenoble. Investigations of alternative ways for electron detection are motivated due to the fact that with MWPCs not every geometric arrangement of the electron detectors which would give us certain advantages can be realised. In 2002 we investigated phoswich detectors as an attractive possibility for electron detection coming along with gamma suppression and low on-the-fly scattering propability for the electrons due to absence of the counting gas.

In principle, a thin scintillator (typical 0.5mm) replaces the signal of the MWPC, providing a Delta E information for charged particles. For gammas, the thin scintillator is nearly insensitive. This layer is mounted on a thick scintillator, wherein charged particles and gammas deposite their energy. The two scintillators have different light decay time constants. The integration of the signal within two time intervals (according to the different time constants of the scintillators) distinguishes electrons from gammas due to the different interaction processes of the particles. The spectrum of a 207Bi source (conversion electrons, two peaks at 475 keV and 980 keV) was recorded with a phoswich setup consisting of two scintillators : BC 404 0.5mm thickness 2ns decay constant, BC 444 10mm thickness, 280ns decay constant. Figures 1a and 1b show the PHD without and with taking advantage of the thin scintillator. For spectrum 1b the coincidence with the thin layer was required within a certain energy interval Delta E. The spectrum could be measured without gamma background down to 120 keV.

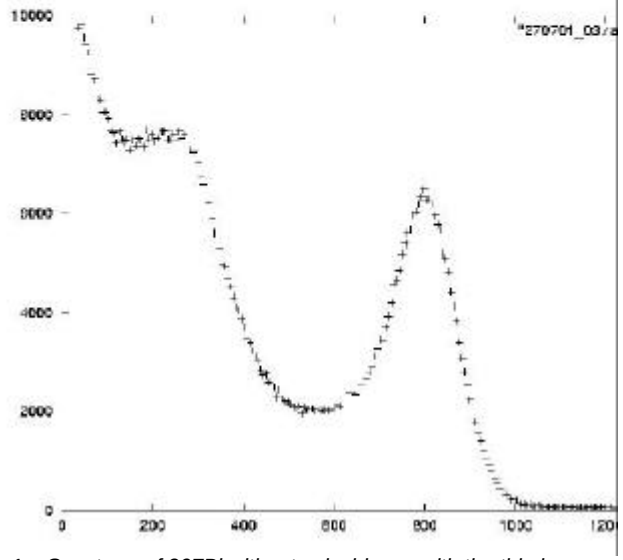

Fig 1a: Spectrum of 207Bi without coincidence with the thin layer

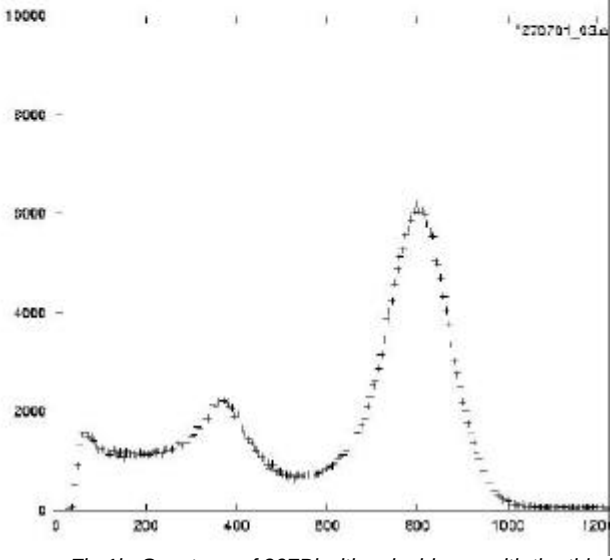

Fig 1b: Spectrum of 207Bi with coincidence with the thin layer

4 POSITRON RESEARCH

4.1 POSITRON SOURCE BASED ON THERMAL NEUTRON CAPTURE AT THE ILL

C. Hugenschmidt[1], G. Kögel[2], R. Repper[1], K. Schreckenbach[1], P. Sperr[2], W. Triftshäuser[2]

[1] Physikdepartment E21, Technische Universität München, Lichtenbergstraße, D-85747 Garching

[2] Institut für Nukleare Festkörperphysik, Universität der Bundeswehr München, D-85577 Neubiberg

A positron beam based on pair production after absorption of high energy prompt γ-rays from thermal neutron capture in ^{113}Cd was installed at PF1. For this purpose, a cadmium sheet (6x12 cm^2, 1.5 mm thick) was placed at the end of the neutron guide in order to generate high intense γ-radiation. The positron source that consists of annealed platinum foils as γ-e^+e^- -converter and as positron moderator was mounted on a removable support in an evacuated beam tube just behind the cadmium sheet. Due to the negative positron work function moderation in heated platinum leads to emission of monoenergetic positrons. After acceleration to 3 keV by four electrical lenses the beam was magnetically guided in a solenoid field of 7.5 mT leading to a NaI-detector in order to detect the 511 keV γ-radiation of the annihilating positrons (fig. 1).

In order to improve the yield of moderated positrons various designs were theoretically optimised by simulating positron trajectories dependent on geometry, electric and magnetic field configuration. In these calculations, important boundary conditions, e.g. emission rate of moderated positrons, asymmetries of the source geometry and energy dependent positron scattering, could not be taken into account quantitatively. Therefore, measurements were performed for various source geometries, dependent on converter mass, moderator surface, acceleration potentials and magnetic compensation coils. The energy distribution of the moderated positrons and degradation of the moderator due to surface contamination were studied as well.

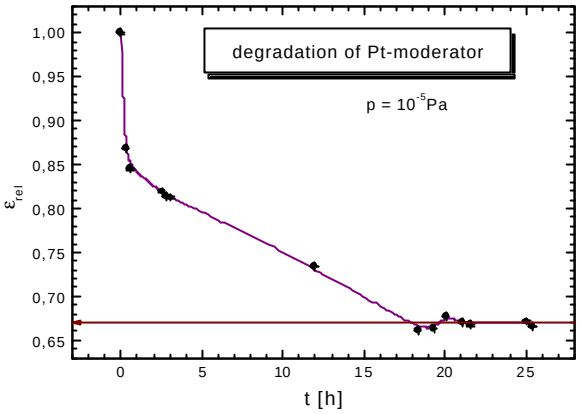

Fig. 1: Decrease of the positron moderation efficiency

With one dedicated geometry the positron beam with a diameter of less than 20 mm yielded an intensity of $3.1 \cdot 10^4$ moderated positrons per second. For polycrystalline platinum the value of the positron work function was found to be -1.95(5) eV. Within the first 20 h of operation a degradation of the moderation efficiency of 30% was observed (fig. 2). An annealing procedure at 873 K in air recovers the platinum moderator.

The results serve as a guideline for the final design of the in-pile positron source at FRM-II.

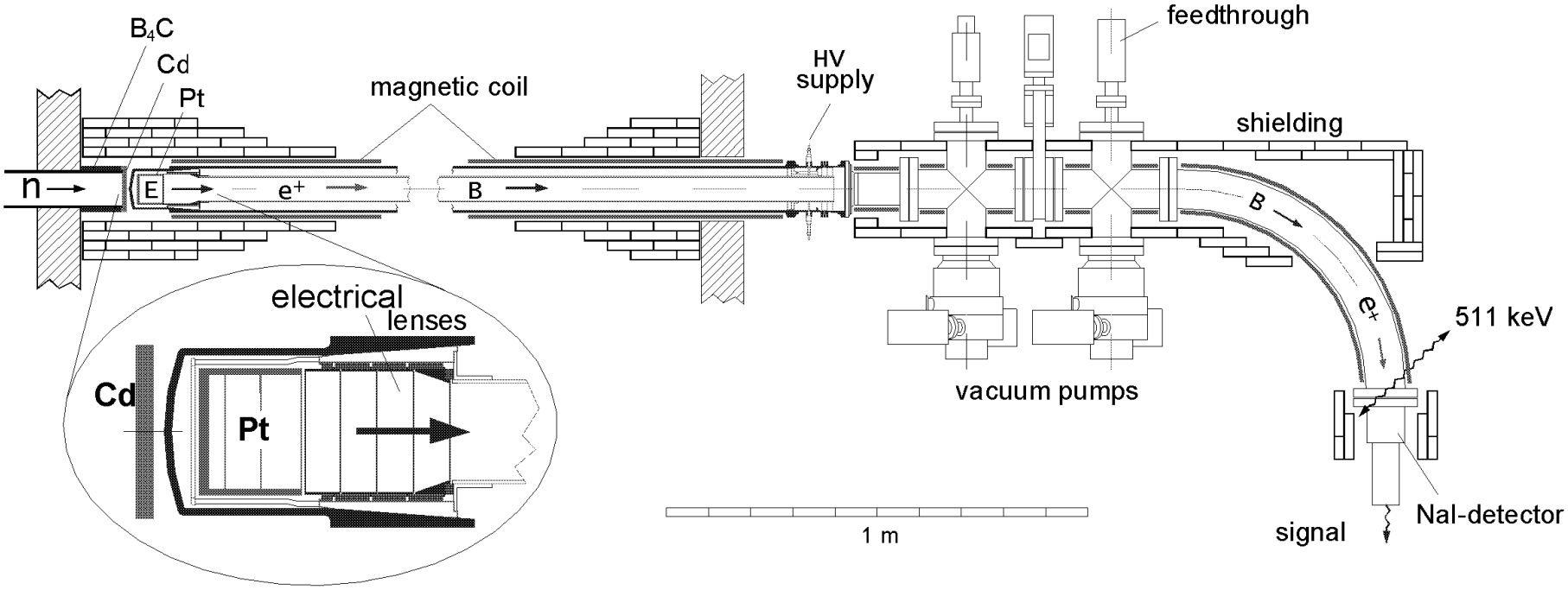

Fig. 2: Experimental set-up of the positron source at PF1 at ILL.

4.2 SLOW POSITRON BEAM FOR AUGER SPECTROSCOPY

B. Straßer, C. Hugenschmidt and K. Schreckenbach
Fakultät für Physik E21, Technische Universität München,
D-85748 Garching, Germany

Auger **e**lectron **s**pectroscopy (AES) is a widespread method in surface physics. Usually, the sample is irradiated with x-rays or keV-electrons to initiate the Auger process by photo- or impact ionisation of core electrons. A commonly measured Auger spectrum shows a high background, caused by secondary electrons which are released by the incoming x-rays or keV electrons. An alternative technique to induce core shell ionisation is the annihilation of core electrons with slow positrons which are focused onto the sample. Due to the low energy (some 10 eV) of the implanted positrons, no background of secondary electrons is produced in the higher energy range of released Auger electrons [1]. Moreover, **p**ositron induced **A**uger **e**lectron **s**pectroscopy (PAES) is much more surface sensitive than classic Auger spectroscopy, since most of the implanted positrons annihilate with electrons of the topmost atomic layer. A PAES-facility basically consists of a slow positron beam, a beam guiding system and an analysis chamber where the positron beam is focused onto a sample. There, the generated Auger electrons are detected by an energy analyser.

At the new research reactor FRM II of the Technical University of Munich, an in-pile intensive slow positron source is currently built up [2]. There, neutron capture gamma rays created by $^{113}Cd(n,\gamma)^{114}Cd$ generate positrons by pair production [3]. One of the first planned experiments at this new positron source is PAES. In order to test a PAES-facility independently from the reactor based positron source, a simple slow positron beam was built up. As β^+ emitter, a 5 mCi ^{22}Na source is used. Behind it, an annealed tungsten moderation foil is mounted, in which the primary positrons are slowed down to thermal energy in transmission geometry. Subsequent electric lenses accelerate the moderated positrons up to desired energy of some 10 eV into beam direction. A longitudinal magnetic field of 2 mT guides the positrons along the curved beamline to the entrance of the analysis chamber, where a μ-metal structure is installed to extract the positron beam out of magnetic guide field. After that, the positrons are electrically focused onto the sample.

During the last year, the mentioned μ-metal structure was constructed and installed. A system of electric beam focus lenses was designed and applied voltages were optimized. The intensity of the slow positron beam was quantified by measuring the 511 keV-line of the positrons annihilating in a beam catcher at the end of the beamline respectively at the sample inside the analysis chamber. The optimized setting of magnetic compensation fields yields an intensity of about $2 \cdot 10^4$ slow positrons per second. The beam profile was studied by a space-resolving micro channel plate detector; a beam diameter of about 5 mm was determined. Furthermore, the beam profile was measured by decrease of the annihilation rate at the sample when it is gradually pulled out of the positron beam. A specific sample mounting was constructed, which allows to anneal the sample “in-situ” inside the analysis chamber. An argon ion sputter gun was installed for sample preparation. Classic, **e**lectron induced **A**uger **e**lectron **s**pectroscopy (EAES) on tungsten and copper was made. Recently, PAES spectra on annealed copper were measured.

REFERENCES

[1] A. Weiss, R. Mayer, M. Jibaly, C. Lei, D. Mehl, K. G. Lynn,
Phys. Rev. Lett. 61 (1988) 2245

[2] C. Hugenschmidt, G. Kögel, K. Schreckenbach, P. Sperr, B. Straßer, W. Triftshäuser,
Mater. Sci. Forum 363-365 (2001) 425

[3] B. Krusche and K. Schreckenbach, Nucl. Instr. Meth. Phys. Res. A295 (1990) 155

5 REACTOR PHYSICS

5.1 ANNUAL REPORT

K. Böning
Fakultät für Physik E21, Technische Universität München

My activities during the years 2000 and 2001 were essentially determined by the ongoing construction and the nuclear licensing procedure of the new high flux research reactor FRM-II. The following main topics can be identified:

1. Contributions to the general management of the FRM-II project with emphasis on questions involving nuclear aspects or reactor physics: properties of the fuel element, required enrichment of the uranium in the fuel element as a function of the available fuel, requirements concerning the purity of the heavy water, planning of the first transports of fuel elements and of the heavy water inventory, exclusion of a recriticality of the unconditioned spent fuel elements in a final geological repository also considering accident scenarios, etc.

2. Preparation of licensing documents and active participation in numerous meetings with representatives of the Bavarian State Ministry of Environmental Protection (StMLU) and its technical experts as part of the nuclear licensing procedure of the FRM-II, after the year of 2000 more and more with the Reactor Safety Commission RSK and the Radiation Protection Commission SSK of the German Federal Ministry of Environment (BMU) and its special technical experts.

3. Technical and scientific assessment of the final report of the experts' commission as established by the German Federal Ministry of Education and Research (BMBF) to investigate the possibility to convert the FRM-II from the use of highly enriched uranium (HEU) to low enriched uranium (LEU). Professional assistance to the Bavarian State Ministry of Science and Research (StMWFK) to support the negotiation of an agreement between the State and the Federal Governments to convert the FRM-II later to the use of medium enriched uranium (MEU). Preparation of the foundation of an international working group to develop such a new fuel element with MEU fuel but unchanged external dimensions.

4. Assistance to develop an international safeguards concept for the fuel elements of the FRM-II by EURATOM and the International Atomic Energy Agency IAEA with participation of the competent German Federal Authorities (BMWi). This included the preparation of documents and the participation in numerous meetings in order to arrive at a well balanced concept which not only fulfils the international requirements of safeguard but also makes sure that the future operation of the FRM-II will not be rendered unnecessarily complicated.

5. Providing information and supporting public relations by performing professional tours of the FRM-II and giving seminars for the representatives of the Bavarian State and German Federal Governments, for the technical assessors, for scientists, and for the interested public.

6 ACTIVITIES 2001

6.1 PUBLICATIONS 2000/2001

1. P. Allenspach, P. Böni, K. Lefmann, "Loss Mechanisms in Supermirror Neutron Guides", SPIE Vol. 4509, (2001) 157-165

2. H. Aschauer, A. Fleischmann, C. Schanzer, E. Steichele, "Neutron guides at FRM-II", Physica B 283 (2000) 323-329

3. A. Axmann, K. Böning, M. Nuding, H.-J. Didier: „FRM-II Status of Construction, Licensing and Fuel Tests“. Proceedings of the 5th International Topical Meeting on Research Reactor Fuel Management (ENS RRFM 2001), Aachen, Germany, 01. – 03. 04.2001, (2001) 1 – 5

4. K. Bodek, P. Böni, C. Hilbes, J. Lang, M. Lasakov, M. Lüthy, S. Kistrin, M. Markiewicz, E. Medvedev, V. Pusenkov, A. Schebetov, A. Serebrov, J. Sromicki, A. Vassiljev, "New Facility for Particle Physics with Polarized Cold Neutrons", Neutron News 11, (2000) 29-31

5. P. Böni, "Novel Concepts in Neutron Instrumentation", Physica B 276-278, (2000) 6-11

6. P. Böni, A. Furrer, "Introduction to Neutron Scattering", in ‘Frontiers of Neutron Scattering’, Proceedings of the 7th Summer School on Neutron Scattering, edited by A. Furrer (World Scientific, Singapore, 2000), (2000) 1-26

7. P. Böni, A. Furrer, J. Schefer, "Principles of Neutron Scattering", in ‘Neutron Scattering in Novel Materials', Proceedings of the 8th Summer School on Neutron Scattering, edited by A. Furrer (World Scientific, Singapore, 2000) (2000), 1-21

8. K. Böning: „IGORR8: Weltkonferenz zu Forschungsreaktoren in München“, Internationale Zeitschrift für Kernenergie ATW, 46. Jahrgang, Heft 6 (Juni 2001), 411

9. K. Böning: „Uran hoher Anreicherung am FRM-II“, Internationale Zeitschrift für Kernenergie ATW, 46. Jahrgang, Heft 11 (November 2001), 705 – 706

10. G.S. Case, M.F. Thomas, C.A. Lucas, D. Mannix, P. Böni, S. Tixier, S. Langridge, "Magnetic Anisotropy in Ce/Fe and Ce/FeCoV Multilayers", J. Phys. Condens. Matter 13, (2001) 9699-9712

11. E.S.Clementyev et al., "Phonon density-of-states in the new superconductor MgB_2", Eur. Phys. J. B 21, (2001) 465

12. F. Demmel, A. Diepold, Chr. Morkel, “The Temperature Dependence of the Shear Modulus in the simple liquid Rubidium”, Physica B 276 – 278, (2000) 456

13. F. Demmel, Ph. Bernhardt, A. Magerl, E. Steichele, "Intensity optimization of a high-resolution ToF diffractometer ", Nuclear Instruments and Methods in Physics Research A 459 (2001) 265 – 272

14. W. Gläser, "Neutronenforschung in Garching“, Technik in Bayern/Hessen 6/2000, (2000) 38 – 39

15. W. Gläser, "Neutronen“, Enzyklopädie Naturwiss. u. Technik – 6. Erg.-Lfg. 2/01, (2000) 1 – 9

16. W. Gläser, “The Future Role of Research Reactors”, Proceedings of the 8th Meeting of the International Group on Research Reactors (IGORR8), Munich, Germany, 17.–20.04.2001, (2001) 2534

17. W. Gläser, “Die zukünftige Rolle von Forschungsreaktoren“, ATW 46. Jg. Heft 6 – Juni, (2001) 413 – 416

18. W. Gläser, Gert v. Hassel, “FRM II: Germany in the Process of Commissioning its New Reactor”, Nuclear Europe Worldscan 1 – 2, (2001) 32

19. W. Gläser, Gert v. Hassel, “Neutronenforschung und wissenschaftliche Projekte“, Forschung in Bayern, Bayerisches Staatsministerium für Wissenschaft, Forschung und Kunst, (2001) 47 – 49

20. T.Herrmannsdorfer, E.S.Clementyev et al., "Magnetic ordering and crystalline electric field splitting in $Nd_3Pd_20Si_6$", J. of Alloys and Comp. 323-324, (2001) 509

21. Hugenschmidt, G. Kögel, K. Schreckenbach, P. Sperr, B. Straßer, W. Triftshäuser, "Intense Positron Source at the Munich Research Reactor FRM-II", Mat. Sci. Forum 363-365 (2001) 425-429

22. Hugenschmidt, G. Kögel, K. Schreckenbach, P. Sperr, B. Straßer, W. Triftshäuser, "Intense Positron Source at the Munich Research Reactor FRM-II", Proc. of IGORR-8 International Group on Research Reactors (2001) 139-142

23. M. Kenzelmann, A. Zheludev, S.Raymond, E. Ressouche, T. Masuda, P. Böni, K. Kakurai, I. Tsukada, K. Uchinokura, R. Coldea, "Spin Waves and Magnetic Ordering in the Quasi-one-dimensional S = ½ Antiferromagnet $BaCu_2Si_2O_7$", Phys. Rev. B 64, (2001) 054422

24. G. Markandeyulu, V.R. Shah, Rama Rao, K.V.S., M.Q. Huang, K. Sirisha, McHenry, M.E. Ramanan, V.R.V, "Anisotropy and FOMP in (SmxPr1-x)3Fe27.5Ti1.5 (x=0-1) and Pr3(Fe1-yCoy)27.5Ti1.5 (y=0-0.4) compounds", IEEE Transactions on Magnetics, Vol. 37 (2001) 2615

25. M. Matsuda, Y. S. Lee, M. Greven, M. A. Kastner, R. J. Birgeneau, K. Yamada, Y. Endoh, P. Böni, S.-H. Lee, S. Wakimoto, and G. Shirane, "Freezing of Anisotropic Spin Clusters in $La_{1.98}Sr_{0.02}CuO_4$", Phys. Rev. B 61, (2000) 4326-4333

26. T. Lehnert, H. Grimmer, P. Böni, M. Horisberger, R. Gotthardt, "Characterization of Shape-Memory Alloy Thin Films Made up of Sputter-Deposited Ni/Ti Multilayers", Acta mater. 48, (2000) 4065-4071

27. M. Nuding, M. Rottmann, A. Axmann, K. Böning: „FRM-II Project Status and Safety of its Compact Fuel Element“. Proceedings of the 4th International Topical Meeting on Research Reactor Fuel Management (ENS RRFM 2000), Colmar, France, 19. – 21. 03. 2000 (2000) 42 – 47

28. M. Nuding, K. Böning: „Irradiation Testing of U_3Si_2-Al Fuels up to Very High Fission Densities“. Proceedings of the 8th Meeting of the International Group on Research Reactors (IGORR8), Munich, Germany, 17. – 20. 04. 2001, (2001) 273 – 280

29. M. Nuding, K. Böning: „Bestrahlungstests an U_3Si_2-Al Brennstoffen bis zu sehr hohen Spaltungsdichten“. Internationale Zeitschrift für Kernenergie ATW, 46. Jahrgang, Heft 6 (Juni 2001), 417 – 419

30. C. Pappas, G. Kali, P. Böni, R. Kischnik, L. A. Mertens, P. Granz, F. Mezei, "The Novel Multidetector Neutron Spin Echo Spectrometer SPAN at BENSC", Physica B 276-278, (2000) 162-163

31. C. Pappas, G. Kali, T. Krist, P. Böni, and F. Mezei, "Wide Angle NSE: the multidetector spectrometer SPAN at BENSC", Physica B 283, (2000) 365-371

32. Yu. V. Petrov, M. S. Onegin, K. Böning, M. Nuding: „Heterogeneous Effects at FRM-II“. Proceedings of the 8th Meeting of the International Group on Research Reactors (IGORR8), Munich, Germany, 17. – 20. 04. 2001, (2001) 259 – 264

33. Yu. V. Petrov, M. S. Onegin, K. Böning, M. Nuding: „Heterogeneous Calculations of FRM-II“. Russian Academy of Sciences, Petersburg Nuclear Physics Institute (PNPI), Preprint 2455, Gatchina-2001 (2001) 24 pages

34. W.-C. Pilgrim, S. Hosokawa, Chr. Morkel, “Density Dependent Atomic Motion in a Liquid Alkali Metal”, Contrib. Plasma Phys. 41, (2001) 283

35. W.-C. Pilgrim, Chr. Morkel, “Diffusion in a Simple Liquid Beyond Brownian Motion”, published as a Highlight in the ILL Annual Report (2001)

36. B. Roessli und P. Böni, "Spin Excitations in Localized and Itinerant Magnets", in `Neutron Scattering in Novel Materials', Proceedings of the 8th Summer School on Neutron Scattering, edited by A. Furrer (World Scientific, Singapore, 2000), (2000) 219-251

37. C. Schanzer, E. Steichele, K. Böning, W. Petry: “Neutronenleitersysteme am FRM-II jenseits der Totalreflexion“. Jahrestagung Kerntechnik 2001, Dresden,15. – 17. 05. 2001, Tagungsbericht ISSN 0720-9207, (2001) 621 – 624

38. K. Schreckenbach, “Nuclear and Particle Physics with Slow Neutrons”, Proc. of the ILL millennium symposium & European user meeting, 6. – 7. April 2001, Grenoble, France, (2001) 29 – 32

39. W. Schweika and P. Böni, "The Instrument DNS: Polarization Analysis for Diffuse Neutron Scattering", Physica B 297, (2001) 155-159

40. F. Semadeni, A. Amato, B. Roessli, P. Böni, C. Baines, T. Masuda, K. Uchinokura, G. Shirane, "Macroscopic and local magnetic moments in Si-doped $CuGeO_3$ as determined by neutron and μSR studies", Eur. Phys. J. B 21, (2001) 307-311

41. F. Semadeni, J. Kohlbrecher, P. Böni, "Spin Dynamics in Ni with SANS: Dipolar Effects and Parallel Fluctuations", Physica B 276-278, (2000) 646-647

42. F. Semadeni, B. Roessli, P. Böni, P. Vorderwisch, T. Chatterji, "Critical fluctuations in the weak itinerant ferromagnet Ni_3Al: A comparison between self-consistent renormalisation and mode-mode coupling theory", Phys. Rev. B 62, (2000) 1083-1088

43. F. Semadeni, B. Roessli, P. Boeni, "Three-axis Spectroscopy with Remanent Benders", Physic B 297, (2001) 152-154

44. M. Senthil Kumar, P. Böni, D. Clemens, "Interface Roughness in Ni/Ti Multilayers as Probed by Neutrons", Physica B 276-278, (2000) 142-143

45. T. Soldner, L. Beck, C. Plonka, K. Schreckenbach, O. Zimmer, “Test of Time Reversal Invariance in Neutron Decay”, Proc. of the ILL millennium symposium & European user meeting, 6. – 7. April 2001, Grenoble, France, (2001) 233 – 235

46. E. Steichele, C. Schanzer, “Design and Set up of the Neutron Guides at FRM –II”, Proceedings of the 8^{th} Meeting of the International Group on Research Reactors (IGORR8), Munich, Germany, 17. – 20. 04.2001, (2001) 2534

47. B. Straßer, C. Hugenschmidt, and K. Schreckenbach, "Set-Up of a Slow Positron Beam for Auger Spectroscopy", Mat. Sci. Forum 363-365, (2001) 686-688

48. K. Uchinokura, Y. Uchiyama, T. Masuda, Y. Sasago, I. Tsukada, A. Zheludev, T. Hayashi, N. Miura, and P. Böni, "Phase Diagram of Spin-Vacancy-Induced Antiferromagnetism in a New Haldane Compound $PbNi_2V_2O_6$", Physica B 284-288, (2000) 1641-1642

49. V.A. Ulyanov, P. Böni, V.N. Khamov, S.P. Orlov, B.G. Peskov, N.K. Pleshanov, V.M. Pusenkov, A.F. Schebetov, A.P. Serebrov, P.A. Sushkov and V.G. Syromyatnikov, "The Effect of Large Irradiation Doses on Polarizing and Non-polarizing Supermirrors", Physica B 297, (2001) 155-159

50. A. Zheludev, T. Masuda, I. Tsukada, Y. Uchiyama, K. Uchinokura, P. Böni, S.-H. Lee, "Magnetic Excitations in Coupled Haldane Spin Chains near the Quantum Critical Point", Phys. Rev. B 62, (2000) 8921-8930

6.2 LECTURES, COURSES AND SEMINARS

M. Bleuel:	Tutorial "Experimentalphysik 1 für Bauwesen" Tutorial "Experimentalphysik 2 für Bauwesen"
P. Böni:	Lectures "Experimentalphysik 1 für Bauwesen" Lectures "Experimentalphysik 2 für Bauwesen" Seminar "Neutrons in Research and Industry"
K. Böning:	Seminar "Special Problems of Nuclear Solid State Physics" Seminar "Neutrons in Research and Industry"
R. Georgii:	Seminar "Neutrons in Research and Industry"
F. Grünauer:	Tutorial "Experimentalphysik 1 für Bauwesen" Tutorial "Experimentalphysik 2 für Bauwesen"
N. Kardjilov:	Tutorial "Elektronikpraktikum"
T. Keller:	Tutorial "Elektronikpraktikum"
Ch. Plonka:	Tutorial "Experimentalphysik 2 für Bauwesen"
S. Prokudaylo:	Tutorial "Experimentalphysik 1 für Bauwesen"
B. Schillinger:	Tutorial "Elektronikpraktikum"

6.3 COMMITTEE MEMBERSHIPS

P. Böni
- Convenor ENSA Working Group “Neutron Optics“
- International Conference on Neutron Scattering ICNS 2001, Munich 2001: International Advisory Committee
- Nutzerausschuss deutsches Kontingent, Institut Laue Langevin, Grenoble
- Instrument Subcommittee, Institut Laue Langevin, Grenoble
- SINQ Scientific Committee
- Projektbegleitender Beirat FRM-II
- Instrumentierungsausschuss FRM-II
- Direktorium FRM-II

K. Böning:
- Chairman (President) of the International Group on Research Reactors IGORR
- Member of the Technical Review Committee (TRC) of the Taiwan Research Reactor System Improvement and Utilization Promotion Project (TRR-II).
- Member of the Scientific Committee of the ENC (European Nuclear Conference) of the European Nuclear Society ENS, Track Leader (together with Alain Ballagny, CEA, France) for „Experimental, Research Reactors and Neutron Sources“ at the ENC 2002 Scientific Seminars
- Projektbegleitender Beirat FRM-II

W. Gläser:
- Direktorium FRM-II
- Instrumentierungsausschuss FRM-II
- Projektbegleitender Beirat FRM-II
- Komitee Forschung mit Neutronen

A. Mirmelstein:
- Member of the International Advisory Committee, International Conference on Neutron Scattering, ICNS 2001, Munich, 9-13 September 2001

B. Schillinger:
- Co-Chairman of the European Society for Neutron Radiology
- Board member of the International Society for Neutron Radiography
- Delegate for the IAEA as Neutron Radiography Specialist

E. Steichele:
- International Conference on Neutron Scattering ICNS 2001, Munich 2001: International Advisory Committee
- Instrumentierungsausschuss FRM-II

6.4 E21 MEMBERS

Name	Phone +49-89-289-	Fax	Room	email
Arend Nikolas, Dipl. Phys.	-14723	-	PH 1, 2205	Nikolas.Arend@frm2.tum.de
Axtner Markus	-12125	-13776	RS, 140	maxtner@ph.tum.de
Bleuel Markus, Dipl. Phys.	-13777	-13776	RS, 124	mbleuel@ph.tum.de
Böni Peter, Prof. Dr.	-14711	-14713	PH 1, 2215	peter.boeni@ph.tum.de
Böning Klaus, Prof. Dr.	-12150	-12191	FRM-II UBA 0325	kboening@frm2.tum.de
Brunner Johannes, Dipl. Phys.	-12106	-13776	RS, 102	brunnerj@ph.tum.de
Clementyev Evgeni, Dr.	-14722	-14713	PH 1, 2207	eclement@ph.tum.de
Gläser Wolfgang, Prof. emerit.	-12476	-12474	PH 1, 2227	wglaeser@ph.tum.de
Grünauer Florian, Dipl. Phys.	-12125	-13776	RS, 140	fgruenau@ph.tum.de
Hils Thomas, Dr.	-14721	-	Flachbau, 17	thomas.hils@hils-consult.de
Kardjilov Nikolay, Dipl. Phys.	-12106	-13776	RS, 102	nikolay@ph.tum.de
Mirmelstein Alexey, Dr.	-14718	-14713	PH 1, 2207	alex.mirmelstein@ph.tum.de
Plonka Christian, Dipl. Phys.	-12299 -12199	-13776	Flachbau, 13	cplonka@ph.tum.de
Prokudaylo Sergey, Dipl. Phys.	-13777	-13776	RS, 124	sprokuda@ph.tum.de
Reich Christian, Diplomand	12515	-	PH I, 2373	creich@ph.tum.de
Russ Barbara, Dipl. Ing.	-14717	-14713	PH 1, 2207	barbara.russ@ph.tum.de
Schanzer Christian, Dipl. Phys.	-14725	-	PH 1, 2214	cschanze@ph.tum.de
Schreckenbach Klaus, Prof. Dr.	-12183	-12191	RS	Klaus.Schreckenbach @Physik.TU-Muenchen.DE
Skorski Cornelia, Sekretaerin	-14712	-14713	PH 1, 2217	cskorski@ph.tum.de
Stadler Christoph, Diplomand	-	-	-	-
Steichele Erich, Dr.	-12141	-12112	RS	esteich@ph.tum.de
Strasser Benno, Dipl. Phys.	-12137	-12191	RS	bstrasse@ph.tum.de
Tejic Daniel	-12656	-	FB PH. T. ABT, 1321	-
Valloppilly Shah, Dr.	-14723	-14713	PH 1, 2205	shah@ph.tum.de
Weiss Verena, Dipl. Phys.	-12515	-	PH 1, 2373	vweiss@frm2.tu-muenchen.de
Wieschalla Nico, Diplomand	-12111	-13776	RS 146b	nico@ph.tum.de

PH: Physics Department
RS: Reactor Station

6.5 ASSOCIATED MEMBERS AT FRM-II

Name	**Phone** Phone: +49-89-289-	**Room**	**email**
Calzada Elbio, Dipl. Ing.	-14611	RS	ecalzada@ph.tum.de
Georgii Robert, Dr.	-14986	RS	robert.georgii@frm2.tum.de
Hugenschmidt Christoph, Dr.	-14609	RS, 4	hugen@ph.tum.de
Langenstück Guido, Dipl. Ing.	-14915	-	langenst@frm2.tu-muenchen.de
Schillinger Burkhard, Dr.	-12185	RS	schilli@ph.tum.de

PH: Physics Department
RS: Reactor Station

6.6 GUESTS

Name	**Phone** +49-89-289-	**Room**	**email**
Gähler Roland, Dr.	-12111	RS 146b	rgaehler@ph.tum.de
Keller Thomas, Dr.	-12164	RS, 4	tkeller@ph.tum.de

PH: Physics Department
RS: Reactor Station